Investigation of Drug Partitioning and Transfer between Artificial Membranes Using Different Techniques

Dissertation
zur Erlangung des akademischen Grades
doctor rerum naturalium
(Dr. rer. nat.)

vorgelegt dem Rat der Biologisch-Pharmazeutischen Fakultät
der Friedrich-Schiller-Universität Jena
Jena, 2011

von Hossam Hefesha
geboren in Menofiya, Ägypten

Gutachter:

1. **Prof. Dr. Alfred Fahr**
2. **Prof. Dr. Dagmar Fischer**
3. **Prof. Dr. Heike Bunjes (Technische Universität Braunschweig)**

Date of defence: 3rd March 2011

Only a life lived for others is a life worthwhile.

Albert Einstein (1879-1955)

To spirit of my dad, my mom, my siblings, my wife, and my children

ACKNOWLEDGMENTS

The present thesis has been prepared between January 2007 and October 2010 at the Department of Pharmaceutical Technology, Institute of pharmacy, Friedrich-Schiller-Universität-Jena.

I would like to express my gratitude to my supervisor Prof. Dr. Alfred Fahr for giving me the opportunity to join his working group and to prepare this thesis. I am very thankful for his tutorial guidance and for supporting me to develop both on a personal and a professional level.

I should also express gratitude to Egyptian Government and my university in Egypt, Al-Azhar University- Cairo, for giving me the opportunity to study abroad and for financing me totally for four years.

I appreciated the supervision of Dr. Xiangli Liu for here contribution in HPLC work and abundant discussions.

I would like also to thank Prof. Dr. Sylvio May for his meaningful cooperation and creation of the mathematical model in the appendix.

I would like also to thank Mr. Frank Steiniger (Friedrich-Schiller Universität-Jena) for supporting Cryo-TEM pictures of the liposomes.

I would like to express my thanks to all of my friends and colleagues in the department especially Mr. Alexander Mohn, Mrs. Angela Herre, and Ms. Ranmona Brabetz who helped me whenever it was necessary.

Finally, I give my deepest gratefulness and warm thanks to my mother, siblings, wife, and my sons for their encouragement and support all through the period of my PhD study.

This thesis has been presented and published in parts in:

Publications

Hossam Hefesha, Stephan Loew, Xiangli Liu, Sylvio May and Alfred Fahr. Transfer Mechanism of Temoporfin between Liposomal Membranes (Journal of Controlled Release, in press).

Liu, X., Hefesha, H., Scriba, G. & Fahr, A. Retention behavior of neutral, positively and negatively charged solutes on immobilized artificial membrane (IAM) stationary phase, Helv. Chim. Acta, 91, 1505-1512, 2008 (*Equal contribution as first author*).

Liu, X., Hefesha, H., Tanaka, H., Scriba, G. & Fahr, A. Lipophilicity Measurement of Drugs by Reversed Phase HPLC over Wide pH Range Using an Alkaline-Resistant Silica-Based Stationary Phase, XBridge^{TM} Shield RP_{18}, Chem. Pharm. Bull., 56, 1417-1422, 2008 (*Equal contribution as first author*).

Congresses:

Hossam Hefesha and Alfred Fahr, Cholesterol transfer (exchange) between liposomal membranes. Controlled Release Society (CRS) German Chapter annual Meeting, Halle (Saale), March 19th-20th, 2009.

Hossam Hefesha, Xiangly Liu, and Alfred Fahr, Kinetics of a hydrophobic drug (temoporfin; mTHPC) transfer between liposomal membranes. Deutschen Pharmazeutischen Gesellschaft (DPhG), Jena, September 28th-1st October, 2009.

ABSTRACT

Drug membrane interactions play an important role in drug transport, distribution, accumulation, efficacy, and resistance. Thus, the measure of drug-membrane partitioning, expressed here as lipophilicity, is one of the most important physicochemical parameters in predicting and interpreting membrane permeability. The partitioning of the drug depends on both the properties of the membrane and the structural and physicochemical properties of the drug. As most drugs are administered via the oral route, the drug has to overcome the epithelial barriers in the stomach and intestinal tract. Therefore, one of the most important factors influencing oral absorption is the permeability of the monolayer of the intestinal epithelial cells lining the gastrointestinal tract. As well, the understanding of the mechanism and the factors influencing the drug release from the drug delivery system and transfer to the site of the action to be up taken by the body cells is prerequisite for drug formulation. Thereby, the partitioning of structurally diverse compounds using different artificial membranes had been investigated. In addition, the factors influencing liposomal formulation of a photosensitizing agent (Temoporfin; mTHPC) and the kinetics of transfer between donor liposomes (drug carrier) and acceptor liposomes (artificial membrane) using the radiolabeled analogue [^{14}C]mTHPC were studied. Two different artificial membranes, immobilized artificial membrane (IAM.PC.DD2) and XBridge^{TM} Shield RP$_{18}$, were chosen using reversed phase high performance liquid chromatography (RP-HPLC). The lipophilicity indices obtained from the two membranes were compared to lipophilicity index of n-octanol/water (log P_{oct}). In terms of mTHPC transfer, to obtain a better insight into the dynamics of mTHPC transfer between membranes, an in vitro model was established. This in vitro model consists of drug incorporation into negatively or positively charged liposomes (donor) and neutral acceptor liposomes which allow the measurement of drug concentration in the acceptor liposomes. Separation of donor and acceptor liposomes of samples taken during the experiments was done by using a mini ion-exchange column. The parameters studied were total lipid content, temperature, charge of donor vesicles, and finally fatty acyl chain structure regarding the length and saturation of phospholipids in donor vesicles.

The results showed significant correlations between the retention factor log k_{wIAM} on IAM.PC.DD2 and log P_{oct} or log $D_{7.0}$ for neutral or structurally related compounds, implying that the retention mechanisms are same among neutral or structurally related compounds. The retention of the ionized compounds on IAM.PC.DD2 is controlled not only by lipophilicity, but also by extra-interactions, mainly electrostatic interactions between charged solutes and

phospholipids. For the solutes investigated on IAM.PC.DD2, positively charged compounds are more retained than negatively charged solutes.

For the Xbridge^{TM} shield RP_{18} phase, it yielded a lipophilicity index log K_w highly correlated with log P_{oct} values for the whole set of compounds investigated. A linear solvation free-energy relationships (LSERs) analysis showed that retention on the Xbridge^{TM} shield RP_{18} phase and partitioning in n-octanol/water are controlled by the same balance of structural properties, namely the Van der Waals volume (V_w), H-bond acceptor basicity (β) and dipolarity/polarizability (π^*). The study showed that the Xbridge^{TM} shield RP_{18} novel stationary phase overcomes the shortcomings of the silica-based stationary phases, whose application in lipophilicity measurements is limited to neutral and acidic compounds.

With respect to mTHPC transfer between liposomal membranes, the obtained results are consistent with a first order kinetics in which the transfer may proceed through liposome collisions or through the aqueous phase. A corresponding theoretical model was presented which accounts for the detailed distribution of drug molecules in donor and acceptor liposomes and predicts the transfer rates as function of drug concentration and number of donor and acceptor liposomes. The experimentally observed transfer rates depended strongly on the temperature and comply with Arrhenius equation. Thermodynamics calculations indicated that the transfer process is entropically controlled. In terms of the charge of donor liposomes, positively charged liposomes showed transfer rate faster than negatively charged liposomes while the maximum amount transferred is almost the same. By investigation of the effect of acyl chain length and saturation of phospholipids of donor vesicles, a potential relationship between transfer rate and membrane rigidity was evident since the transfer rate did sharply increase when the liposomal membranes were rigid at 37 °C.

ZUSAMMENFASSUNG

Wechselwirkungen zwischen Arzneistoffen und Membranen spielen eine wichtige Rolle im Arzneistofftransport, sowie der Verteilung, Anreicherung im Gewebe und der Wirksamkeit. Folglich ist die Verteilung zwischen Arzneimittel und Membran, die hier als Lipophilie ausgedrückt wird, eine der wichtigsten physikochemischen Parameter beim Voraussagen und Interpretieren der Membranpermeabilität. Die Verteilung des Arzneistoffes hängt sowohl vom Aufbau der Membran als auch von strukturellen und physikochemischen Eigenschaften des Arzneistoffes ab. Da heutzutage die meisten Arzneitstoffe oral verabreicht werden, müssen diese die epithelialen Barrieren im Magen und Darmtrakt überwinden. Daher ist die Durchlässigkeit des Monolayers der Darmepithelzellen des Gastrointestinaltraktes einer der wichtigsten Faktoren, der die orale Aufnahme beeinflusst. Eine weitere wichtige Voraussetzung für eine effiziente Arzneistofffomulierung ist das Verständnis für die Mechanismen und Faktoren, die die Arzneistofffreisetzung vom Trägersystem, dessen Transfer zum Wirkort und die Aufnahme in Zellen beeinflussen. Hierfür wurde die Verteilung strukturell unterschiedlicher Verbindungen mittels des Einsatzes verschiedener künstlicher Membranen untersucht. Zusätzlich wurden Faktoren, die die liposomale Formulierung eines photosensiblen Stoffes (Temoporfin; mTHPC) und dessen Transferkinetik zwischen Donorliposomen (Arzneiträger) und Akzeptorliposomen (künstliche Membran) beeinflussen, untersucht. Die Experimente wurden mit dem radioaktiv markierten Analogon [^{14}C]mTHPC durchgeführt. Zwei unterschiedliche künstliche Membranen, die immobilisierte künstliche Membran (IAM.PC.DD2) und XBridge^{TM} Shield RP_{18}, wurden mittels Umkehrphasen-Hochleistungsflüssigkeitschromatografie (RP-HPLC) ausgewählt. Die von den Membranen erhaltenen Lipophilie-Indizes, wurden mit dem lipophilie Index von n-Octanol/Wasser (log P_{oct}) verglichen. Um einen besseren Einblick in die Dynamik des mTHPC Membrantransfers zu gewinnen, wurde ein *in vitro* Modell etabliert. Dieses *in vitro* Modell beinhaltet das Laden von Arzneistoffen in negativ oder positiv geladene Liposomen (Donor) und neutralen Akzeptorliposomen. Im Anschluß ist es möglich, die Arzneistoffkonzentration im Akzeptorliposom zu quantifizieren. Die Trennung der Donor und Akzeptorliposmen erfolgte über eine mini Ionenaustauschersäule. Zu den untersuchten Parametern gehörten der totale Lipidgehalt, Temperatur, Ladung der Donorvesikel, und schließlich die Struktur der Kohlenwasserstoffketten bezüglich ihrer Länge und der Sättigunggrad der Phospholipide in den Donorvesikeln.

Die Ergebnisse zeigten eine signifikante Korrelation zwischen dem Retentionsfaktor log k_{wIAM} von IAM.PC.DD2 und log P_{oct} oder log $D_{7.0}$ für neutral oder strukturell verwandte Zusammensetzungen, was besagt, dass die Retentionsmechanismen bei neutralen oder strukturell verwandten Zusammensetzungen gleich sind. Die Retention von ionischen Zusammensetzungen auf IAM.PC.DD2 wird nicht nur durch deren Lipophilie, sondern auch durch zusätzliche Wechselwirkungen, beeinflusst. Es handelt sich hauptsächlich um elektrostatische Wechselwirkungen zwischen geladenen gelösten Stoffen und Phospholipiden. Unter den auf IAM.PC.DD2 geprüften Verbindungen, wurden positiv geladene Zusammensetzungen stärker zurückgehalten als negativ geladene.

Für die Xbridge^{TM} Shield RP_{18} Phase ergab sich ein Lipophilie-Index log K_w, der eine hohe Korrelation mit den log P_{oct} Werten aller getesteten Verbindungen aufwies. Eine Lineare Freie-Energie-Beziehungs (LSERs) Analyse zeigte, dass die Retention auf der XbridgeTM Shield RP18 Phase und die Verteilung in n-Octanol/Wasser auf der selben Ausgewogenheit struktureller Eigenschaften basieren, im speziellen auf dem Van der Waals Volumen (*Vw*), der H-Brücken Akzeptorbasizität (β) und der Dipolarität/Polarisierbarkeit (π^*). Die Tests haben gezeigt, dass die neue stationäre Xbridge^{TM} Shield RP_{18} Phase die Mängel von auf Kieselgel basierenden stationären Phasen überwinden kann, die nur lipophilie Messungen von neutralen und sauren Verbindungen ermöglichen.

Die erhaltenen Daten des mTHPC Transfers zwischen liposomalen Membranen zeigten, dass der Transfer einer Kinetik erster Ordnung folgt, und möglicherweise durch Zusammenstöße der Liposomen oder über die wässrige Phase erfolgt. Ein entsprechendes theoretisches Modell wurde präsentiert, welches die detaillierte Verteilung von Arzneistoffmolekülen in Donor und Akzeptorliposomen zeigt, und die Transferraten als Funktion von Arzneistoffkonzentration und der Anzahl von Donor und Akzeptorliposomen vorraussagen kann. Die experimentell ermittelten Transferraten waren stark temperaturabhängig und entsprachen der Arrhenius Gleichung. Thermodynamische Berechnungen haben gezeigt, dass der Übertragungsprozess entropisch kontrolliert ist. Bezüglich der Ladung der Donorliposomen, zeigten positiv geladene Liposomen eine schnellere Transferrate als negativ geladene Liposomen, während die maximal übertragene Menge fast dieselbe war. Durch Untersuchung der Kohlenwasserstoffkettenlänge und des Sättigungsgrades der Phospholipide der Donorvesikel konnte eine positive Korrelation zwischen der Übertragungsrate und der Membransteifigkeit nachgewiesen werden.

CONTENTS

ABREVIATIONS

IAM	Immobilized artificial membrane
LSERs	Linear solvation free-energy relationships
QSPR	Quantitative structure permeability relationship
PAMPA	Parallel artificial membrane permeation assay
IL	Immobilized liposomes
MPS	Mononuclear phagocyte system
PS	Photosensitizer
LDL	Low density lipoprotein
mTHPC	Temoporfin
i.v.	Intravenous
PDT	Photodynamic therapy
DPPC	1,2-Dipalmitoyl-sn-glycero-3-phosphocholine
DSPC	1,2-distearoyl-sn-glycero-3-phosphocholine
DMPC	1,2-Dimyristoyl-sn-glycero-3-phosphocholine
DBHPC	1,2-dibehenyl-sn-glycero-3-phosphocholine
DOPC	1,2-dioleoyl-sn-glycero-3-phosphocholine
SOPC	1-stearoyl-2-oleoyl-sn-glycero-3-phosphocholine
DOTAP	1,2-dioleoy-3-trimethylammonium-propane sodium salt
POPC	Palmitoyl-2-oleoyl-3-sn-glycero-3-phosphocholine
Chol	Cholesterol
DCP	Dicetylphosphate
DEAE	Diethylaminoethyl
CM	Carboxymethyl
MLVs	Multilamellar vesicles
MeOH	Methanol
SUV’s	Small unilamellar vesicles
PDI	Polydispersity index
SEM	Standard error mean
PCS	Photon correlation spectroscopy
LSC	Liquid scintillation counting
NSAIDs	Nonsteroidal anti-inflammatory drugs

PART I
INTRODUCTION AND OBJECTIVES

1.1 INTRODUCTION

Concern in drug design has focussed mainly on the interaction of ligand molecules with proteins, in the form of specific receptors and enzymes. Membranes contain most of the target proteins, and it is supposed that the drugs display their action as a result of binding to the membrane-embedded proteins. The lipid part in membrane is well known to play a more passive role. However, there is increasing the opinion that the influence of drug-membrane interaction on drug activity and selectivity has been underestimated in the past. The so-called ‘‘non-specific’’ interaction of drugs with membrane constituents in fact involves an interaction with specific phospholipids structures. Although the lipid layer is a dynamic fluid, it is highly organized. Interaction with the organised phospholipid structures can have a decisive influence on drug partitioning, orientation, conformation, and drug transfer between membranes as well. It also has an effect on the physicochemical properties and functioning of the membrane. Therefore, drug membrane interactions play an important role in drug transport, distribution, accumulation, efficacy, and resistance (*1*). In general, most of drugs reach their target organ via the blood circulation system. As a result, the drug molecules first have to pass through barrier membranes in the gastrointestinal tract to enter the circulation. The partitioning or the transfer of the drug depends on both the properties of the membrane and physicochemical properties of the drug. In addition, the majority of the drugs are administered by the oral route. So, the barrier the drug has to overcome in the stomach and intestinal tract is a monolayer epithelium. Therefore, the main factor influencing oral absorption is the permeability of the monolayer of the intestinal epithelial cells lining the gastrointestinal tract. As the active thransepithelial resorption is the exception rather than the rule, and as no watery pores exist in the intact mucosa, drugs must have certain lipophilic properties if they are to cross the epithelium of the intestine by passive diffusion, including paracellular and transcellular permeation. On the other hand, for the drug partitioning or release from the formula into the watery fluid of the stomach or intestine requires a certain degree of solubility in water. It is therefore accepted and very well known that the percentage absorbed in general follow a non-linear dependency with lipophilicity, normally being expressed as the n-octanol-water partition coefficient (log P_{oct}) (*2*). Whereas molecular volume is the foremost determinant of whether a solute may cross the paracellular pathway (*3, 4*), lipophilicity gives indirect information on how likely that pathway is to play a significant role in bioavailability. In addition, lipophilicity may give indication about substrate-transporter interaction, either by local or global information on substrate hydrophobicity. The importance of drug lipophilicity determination (*5, 6*), however, is that it

directly influences the degree of membrane partitioning and hence passive membrane transport of solutes. In assessment of drug-membrane partitioning, lipophilicity is considered one of the most important physicochemical parameters in predicting and interpreting membrane permeability. The dependence of oral drug absorption on drug lipophilicity was demonstrated (*7*) and implicated an optimal range of partition coefficients for a chemical series (*8*). Later work, in which a model for intestinal absorption potential was derived, defined the critical physicochemical components for absorption as partition coefficient, fraction in non-ionised form at pH 6.5, and the dose-solubility ratio (*9*). The dependence of passive transport on lipophilicity has been also recognized by researchers investigating the permeation of the drugs through the blood-brain barrier (*10-12*). Moreover, numerous studies (*13*) of quantitative structure-permeability relationship (QSPR) have explicitly verified that lipophilicity, as related to membrane partitioning and hence passive transcellular diffusion, is a key parameter in predicting and interpreting permeability. In these studies, lipophilicity is often equated with the n-octanol/water partition coefficient (log P_{oct}) (*13*). The partition coefficient (log P_{oct}) in this solvent system (n-octanol/water) is traditionally accepted as an informative model of membrane partitioning (*14*). As a molecular parameter, lipophilicity encodes both polar and hydrophobic intermolecular forces. But when expressed by partition coefficients measured in traditional organic solvent/water systems, lipophilicity fails to encode some important recognition forces, most notably ionic bonds, which are of particular importance when modelling the interaction of ionized compounds with membranes. And in fact, a recent statistic found that 62.9 % of drugs are ionisable, of which 14.5 % are acids, 67.6 % are bases, and 17.9 % are ampholytes of various types (*13*). So, any prediction of pharmacodynamic and pharmacokinetic properties of the drugs should take their ionization into account since the majority of drugs are ionisable. Therefore, at a pH value where the compounds are ionized, the partitioning values considered are distribution coefficients (log $D_{7.0}$). In the fact, the partition coefficients of compounds between buffers and model membrane phases showed that interactions between charged molecules and biomembranes can be complex and include both polar and hydrophobic interactions. In particular, studies on partitioning behaviour of ionized compounds between two phases, aqueous buffers and phospholipids vesicles (*15*), they found that certain structural patterns in ionized molecules could enhance their partitioning into membrane bilayers. Some of studies were done on a new HPLC stationary phase material composed of monolayer of lethicin, the so-called immobilized artificial membrane (IAM), confirmed these observations for some basic compounds in ionised forms (*16*). Fortunately, the partitioning or transfer of the drug that can

occur in the biological membranes can be studied and simulated in vitro and quantified by available physicochemical techniques, using as a model artificial membranes which are recently created. Despite the reference method to measure log P_{oct} is shake-flask method, it is time consuming, limited in range (-3< log P_{oct} < 4) and outside these limits log P_{oct} values become unreliable (*17*). Hence, during the recent decades, the use of artificial phospholipid membranes as a model for biological membranes becomes the subject of intensive research. As known that biological membranes are composed of complex mixtures of lipids, sterols, and proteins. Therefore, defined artificial membranes may serve as simple models of membranes that have many strong similarities with biological membranes. Artificial membranes are used to study the influence of drug structure and membrane composition on drug partitioning and/or transfer (*18*). The partition, including affinity, location, and specific interaction and diffusion kinetics are the characteristics of membrane permeation with certain phospholipids. Because of the complex events involved during drug absorption in vivo, true membrane permeability modelling cannot always be created. Therefore, many attempts have been made to develop suitable in vitro systems to study the permeation process and its dependence on membrane composition and drug physicochemical properties (*2*). One of these attempts is the cell culture model involving Caco-2 cells, which is a human intestinal epithelial cell line. The membranes of these cells have useful properties for correlation with in vivo data such as enzymatic and transporter systems (*19*). Therefore, this cell line has been proposed and used for the simulation and prediction of intestinal drug absorption after oral administration. Kansy and co-workers developed another system called physicochemical high-throughput screening system (PC-HTS). This model used a parallel artificial membrane permeation assay (PAMPA) for the explanation of passive absorption processes (*20*). PAMPA is based on a 96-well microtiter plate assay that allows the measurements of numerous compounds per day. A planar bilayer membrane of egg phosphatidylcholine-decane, for example, has been used to study the permeation of monocarboxylic acids (*21*). Another model, drug-liposome partitioning, has been described as a tool for the prediction of absorption in the human intestinal tract (*22*). One of the most important chromatographic methods is reversed-phase high performance liquid chromatography (RP-HPLC) where the capacity factor (log K_w) derived from isocratic log K_w values by extrapolation to 100 % water. This method became a well-accepted method for the determination of the lipophilicity (*23-26*). For instance, IAM, fast and reproducible test systems, are used for studying drug-membrane interaction in relation to drug transport. IAM column chromatography becomes even more important in combination combinatorial chemistry and high-throughput screening

methods. The columns are packed with single-chain (IAM.PC) or double-chain phospholipids (IAM.PC.DD and IAM.PC.DD2), in which the chain was linked by ester or ether groups to the glycerol backbone of PC as depicted in figure 1.1. IAM column chromatography has been also used to predict the transdermal transport of drugs (*27*). One more of the attempts of drug partitioning determination systems is the immobilized liposome chromatography (ILC). In this system, the drug partitioning is determined using liposomes or biomembranes immobilized in gel beads by freeze-thawing (*28*). The lipid used can be phosphatidylcholine, phosphatidylserine, egg phospholipid, lipids extracted from human red cell membrane vesicles, vesicles from cytoskeleton-depleted human red cell membrane vesicles, and ghosts from human red cell membranes (*2*).

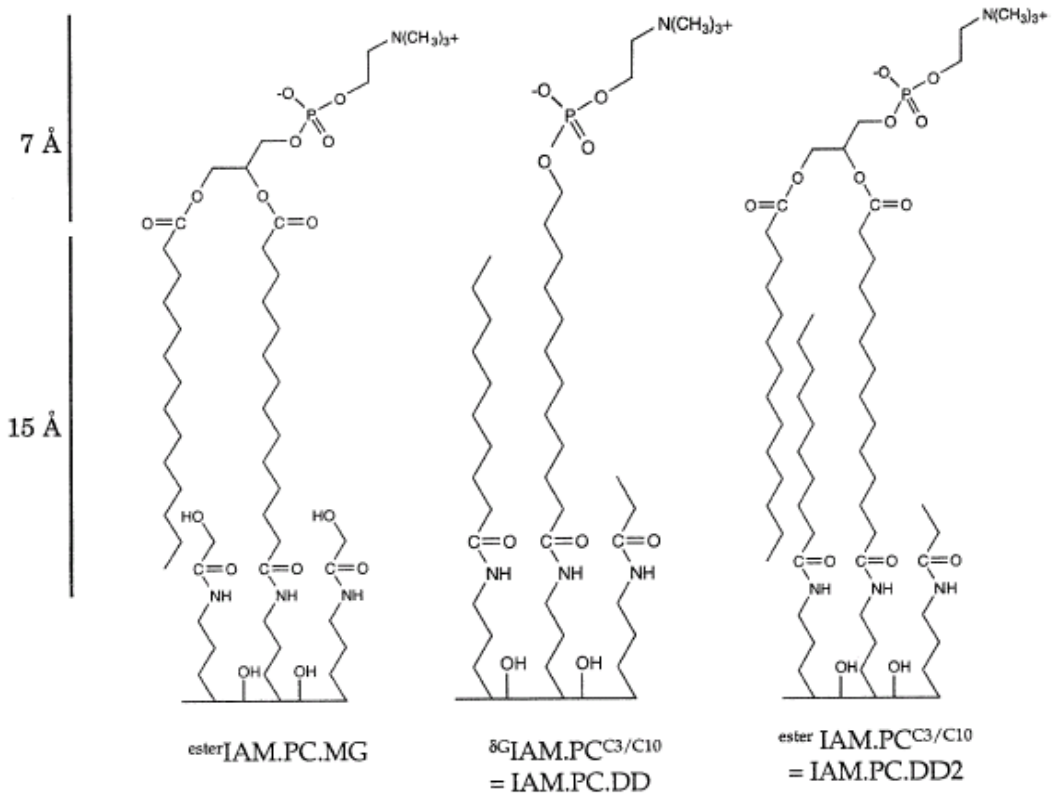

Figure 1.1. Structures of commercially available immobilized artificial membranes (IAM). (Adapted from reference (*13*)).

In addition to the importance of drug partitioning, understanding of the mechanism and the factors influencing the drug release from the drug delivery system and transfer to the site of the action is a prerequisite for drug formulation. Nowadays, a very broad range of drug molecules are currently in use and new drugs are added to the list yearly. Increasing the therapeutic index of the drug and minimizing its side-effects is one of the main goals of any

treatment employing xenobiotics. The clinical use of most conventional chemotherapeutics is limited because of the inability to deliver therapeutic drug concentrations to the target tissues and/or severe and harmful toxic effects on normal organs and tissues. Many approaches have been done to dissolve these problems by providing "selective" delivery to the affected tissues. The ideal drug delivery system would be to bring the drug only to the site of action. This purpose can be achieved by using suitable drug carrier like molecular conjugates and colloidal particulates. Colloidal particulates carriers prepared from physical incorporation of the drug into a particulate colloidal system such as liposomes, niosomes, micro- and nano-spheres, erythrocytes, and polymeric and reverse micelles. Liposomes are one of these carriers which have been most studied. Liposomes are biocompatible and biodegradable which make them interesting for the researchers. They consist of an aqueous core surrounded by one or more bilayers composed of natural or synthetic lipids. Liposomes composed of natural phospholipids are biologically inert and weakly immunogenic, and they possess low intrinsic toxicity. Further, drugs with different lipophilicities can be encapsulated into liposomes: water insoluble drugs are entrapped almost completely in the lipid bilayer, freely water soluble drugs are located exclusively in the aqueous compartment, and sparingly water soluble drugs (with intermediate log P_{oct}) easily partition between the bilayer and the aqueous core (*29*). Liposomal formulations for water insoluble drugs have been developed and successfully introduced into the market (*30, 31*) since the liposomes being used in intravenous rote of administration (*32-34*). The literatures mentioned that conventional liposomes or modified liposomes may change the pharmacokinetic or pharmacodynamic behaviour of the drug. These changes may be ascribed to a modified distribution of the liposomal drug in tissues (*35*). Together with a prolongation of the half-life of the drug, active targeting is achieved (*36, 37*). Also the half-life of liposomes in the blood circulation can be reduced by passive targeting (i.e. spontaneous or opsonin-mediated uptake) to cell of the Mononuclear Phagocyte System (MPS) (*38*). Moreover, direct targeting of the carrier to the site of action in the body could be explored (*39, 40*). All of these approaches are directed to increase the therapeutic index of the liposomal drug. So, the formulation of lipophilic drug in liposomal drug delivery system and the transfer kinetics between membranes is of paramount importance. But, because of numerous complications arise in the investigation of drug transfer in biological systems, due to protein and adsorption of vesicles to membranes, and the complex structures of biological membranes and lipoproteins (*41, 42*), liposomes are the most useful simplified models of biological membrane. As a result, an in vitro model was established (*35, 43*) to obtain a better insight into the dynamics of a drug transfer between

membranes. This in vitro model consists of drug incorporation into negatively or positively charged liposomes (donor) and neutral acceptor liposomes which allow the measurement of drug concentration in the acceptor liposomes. Separation of donor and acceptor liposomes of samples taken during the experiments was done by using a suitable mini ion-exchange column. The principle of this method is shown in figure 1.2. In this model, transfer is typically determined by using of a radiolabeled analogue (*44, 45*). The present study focused on one of few approved porphyrins in cancer therapy to date. Porphyrins with a fully conjugated macrocycle represent the fundamental group of photosensitizers (PS). The main usage of photosensitization is the treatment of different tumor classes which have been found to accumulate certain photosensitizers, especially porphyrins, with some selectivity (*46, 47*). The recent development of diode lasers and optical fibres has facilitated the use of light-sensitive drugs in various therapeutic and experimental applications (*48*). Corresponding techniques are based on irradiation of PS with light, which generates active molecular species such as free radicals and singlet oxygen. These short-lived species are highly toxic in a biological environment (*49*) and exhibit restricted diffusion (*50*). Damage to biomolecules is thus determined by the localization of the photosensitizer at the moment of irradiation. The ionization state and hydrophobicity of the photosensitizer are the main determinants of subcellular localization and, consequently, of photobiological efficacy (*51, 52*). Membrane structures, especially those of mitochondria (*53*), have been found to be particularly sensitive to photosensitization. Most of the currently available PS are amphiphilic or hydrophobic compounds that have a tendency to self-aggregate when injected into a physiological aqueous environment. Therefore, different delivery systems such as liposomes, Cremophor EL, cyclodextrin, or lipoproteins have been employed in order to facilitate the transport of poorly water-soluble PS (*54-57*). The use of specific delivery systems can modulate the pharmacokinetics and cellular uptake of PS. For instance, the administration of porphyrins incorporated into DPPC liposomes enhances the accumulation and prolongs the retention of PS by cultured cells and experimental tumours (*58-60*). Transport mediated by LDL was suggested to enhance the selective accumulation of some PS in the tumour tissue (*55, 61, 62*). The passive cellular uptake of PS and its partition among sub-cellular structures is most likely dominated by the dynamics of its permeation through the membranes. Moan and co-workers (*63*) suggested that the low pH value of the interstitial fluid in tumours favours passive cellular incorporation of carboxylic porphyrins. This hypothesis gained support from studies on the interactions of porphyrins with membrane models (*64*) and from in vivo experiments (*65, 66*). Consistent with this, multiple studies argue that the transport of hydrophobic

compounds between cellular membranes may proceed in the absence of metabolic energy and does not require specific protein or ionic interactions (*35, 43, 67, 68*). In vitro studies have shown also that the translocation of porphyrins within cells is quite fast (*69*). Thus, a precise knowledge of the mechanism and the factors controlling the transfer of PS across membranes will contribute to the design of liposomes as a drug carrier and to the efficacy of drug delivery system, and will consequently improve PDT. However, the complex structure of PS, the large size of its macrocycle, and the asymmetric distribution of side chains around the macrocycle render usual predictions based on octanol/water partitioning difficult (*70*). Moreover, many complications arise in the investigation of passive transport in biological systems (protein, adsorption of vesicles to membranes, and the complex structures of biological membranes and lipoproteins). Therefore, we used mini ion-exchange column in vitro model to study temoporfin transfer between liposomal membranes. Temoporfin is one of porphyrins belonging to the second generation photosensitizers clinically used under the trade name of Foscan® (*71*). Temoporfin (mTHPC) structure is depicted in figure 1.3. After intravenous injection, mTHPC has been shown to be effective in PDT in the treatment of squamous cell carcinoma of head and neck, in the treatment of early or recurrent oral carcinomas, in the palliative treatment of refractory oral carcinomas (*72*) and in the treatment of primary non-melanomatous tumor of the skin of the head and neck (*73*).

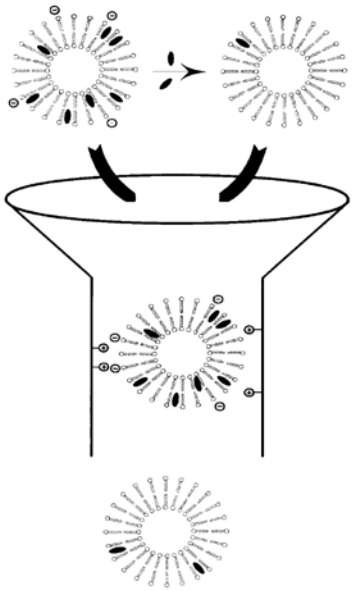

Figure 1.2. Measurement of temoporfin between liposomal membranes. Micro-columns made of Perspex® were filled with DEAE Sepharose^{TM} CL-6B or CM Sepharose^{TM} Fast Flow equilibrated in iso-osmolar sucrose. (Adapted from reference (*74*)).

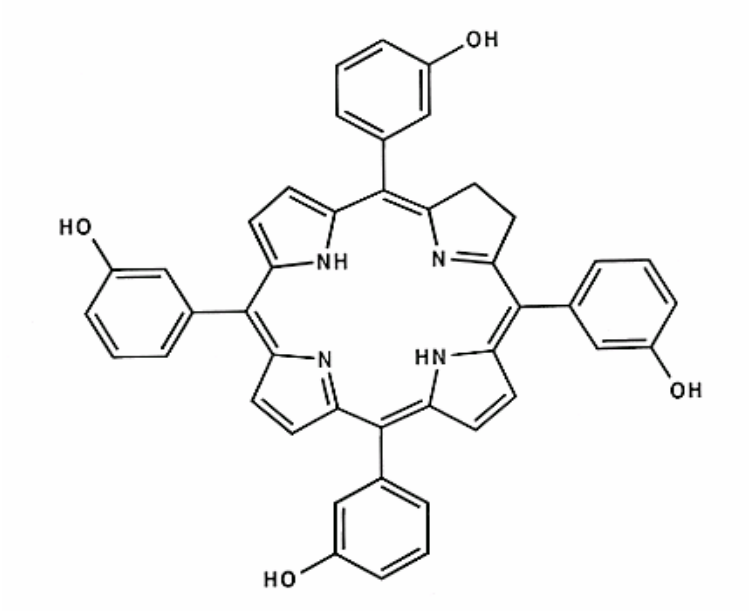

Figure 1.3. Chemical structure of temoporfin.

1.2 OBJECTIVES

As mentioned above, to elicit its pharmacological and therapeutic effects, a drug has to cross various cellular barriers by passive diffusion and/or by carrier-mediated uptake. As a result, drug design and discovery can not have pharmacodynamic efficacy as the sole criterion of optimization but must also take pharmacokinetic considerations into account, in particular absorption and distribution. The importance of drug lipophilicity prediction is that it directly influences the degree of membrane permeability of solutes. A new approach for studying passive absorption and distribution of the drug is based on artificial membranes. Therefore, the aim of this thesis was to investigate the partitioning of structurally diverse compounds including ionized, non-ionised, and zwitterionic species in addition to some drugs using different artificial membranes. Two of artificial membrane models, immobilized artificial membrane (IAM.PC.DD2) and XBridge^{TM} Shield RP_{18}, were chosen using reversed phase high performance liquid chromatography (RP-HPLC). The lipophilicity indices obtained from the two membranes were compared to the lipophilicity index of n-octanol/water (log P_{oct}). In addition to the partitioning studies, the liposomal formulation of a photosensitizing agent (Temoporfin; mTHPC) and the kinetics of transfer between donor liposomes (drug carrier) and acceptor liposomes (artificial membrane) using the radiolabeled analogue [^{14}C]mTHPC have been studied. The influence of total lipid content, temperature, charge of donor vesicles,

and finally fatty acyl chain structure regarding length and saturation of phospholipids in donor vesicles was investigated.

PART II
MATERALS AND METHODS

2. Materials and Methods

2.1 Materials

Acridine, Aniline, N-Ethylamine, 2-Chloroaniline, 2-Aminobiphenyl, Benzyl cyanide, Acetophenone, Nitrobenzene, 1-Chloro-2-Nitrobenzene, Benzyl alcohol, 4-Chloro-Benzyl alcohol, 3-Chlorophenol, 3-Nitrophenol, 3-Phenylpropionic acid, 4-Phenylbutyric acid, 5-Phenylvaleric acid, 8-Phenyloctanoic acid, Benzoic acid, 4-Bromobenzoic acid, 3-Chlorobenzoic acid, 4-Iodobenzoic acid, 1-Naphthoic acid, 4-Methylbenzyl methylamine, 4-Methylbenzyl ethylamine, 4-Methylbenzyl propylamine, 4-Methylbenzyl butylamine, 4-Methylbenzyl pentylamine, 4-Methylbenzyl hexylamine, 4-Methylbenzyl heptylamine, Aspirin, Antipyrine, Mefenamic acid, Flurbiprofen, Indomethacin, Ketoprofen, Naproxen, Phenylbutazone, Promethazine hydrochloride, Metoprolol, Metipranolol, Oxprenolol, Penbutolol, Pindolol, Propranolol hydrochloride, Corticosterone, Estrone, Estradiol, Hydrocortizone, Hydrocortizone-21-acetate, Progesterone, Dexamethazone, Testosterone, Phenytoin, Sulfabenzamide, Sulfacetamide, Sulfamethazine, Sulfamethoxazole, Sulfamethoxypyridazine, Sulfanilamide, Uracil and Citric acid. All former compounds were obtained from commercial sources (Sigma-Aldrich, Steinheim, Germany; Carl Roth, Karlsruhe, Germany; VWR, Leuven, Belgium) in the highest available purity except the (4-methylbenzyl) alkylamines were synthesized by known procedures (*75*). 1,2-Dipalmitoyl-sn-glycero-3-phosphocholine (DPPC) and 1,2-distearoyl-sn-glycero-3-phosphocholine (DSPC) were purchased from Sygena LTD (switzerland). 1,2-Dimyristoyl-sn-glycero-3-phosphocholine (DMPC), 1,2-dibehenyl-sn-glycero-3-phosphocholine (DBHPC), 1,2-dioleoyl-sn-glycero-3-phosphocholine (DOPC), 1-stearoyl-2-oleoyl-sn-glycero-3-phosphocholine (SOPC) and 1,2-dioleoy-3-trimethylammonium-propane sodium salt (DOTAP) were purchased from Avanti Polar Lipids (Alabaster, AL, USA). 1- Palmitoyl-2-oleoyl-3-sn-glycero-3-phosphocholine (POPC) was purchased from Genzyme Pharmaceuticals (Liestal, Switzerland). Meta-tetrahydroxyphenylchlorin (^{14}C-temoporfin; [^{14}C]mTHPC) was kindly provided as a gift from Biolitec AG (Jena, Germany). Cholesterol (Chol), Dicetylphosphate (DCP), Trizma® pre-set crystals and Sodium azide were obtained from Sigma Chemical Co. (St. Louis, MO. USA). Diethylaminoethyl (DEAE) Sepharose™ CL-6B and Carboxymethyl (CM) Sepharose™ Fast Flow preserved in 20% ethanol were purchased from GE Healthcare Bio-Sciences AB (Uppsala, Sweden). Sucrose was purchased from Carl Roth GmbH (Karlsruhe, Germany). Radioactive substances ^{3}H-Cholesteryl-oleate (1mCi/ml) and ^{14}C-Cholesteryl-oleate (100 Ci/ml) were purchased as a stock solution in

toluene solvent from GE Healthcare UK Ltd (Amersham radiochemicals) (Buckinghamshire, UK). Sodium chloride was purchased from Merck KgaA (Darmstadt, Germany).

2.2 METHODS

2.2.1 Immobilized Artificial Membrane Chromatography (IAM.PC.DD2)

2.2.1.1 Determination of Retention Times (t_r)

To measure the capacity factors, a liquid chromatograph was used. The device consisted of a HPLC pump System-Gold-125 solvent module, a System-Gold-507e autosampler, and a System-Gold-UV/VIS-168 detector (all from Beckmann Coulter, Inc., Fuerton, CA, USA). IAM.PC.DD2 (100 mm_4.6 mm i.d., 10 μm) was purchased from Regis Technology (Morton Grove, IL, USA).

2.2.1.2 Mobile Phase and Flow Rate

Two types of mobile phases were used; 1) 0.02M phosphate buffer pH 7.0. 2) 0.02M phosphate buffer pH 7.0 mixed with methanol in proportions varying from 70 to 10% (v/v). Before mixing the phosphate buffer with methanol, phosphate buffer was filtered under vacuum through a HA-Millipore filter (0.45μm; Millipore, Milford, MA, USA). At room temperature and by using the UV/VIS detector at the specific λ_{max} of the each analyte, the retention times were identified. The flow rate of 1.0 ml/min was applied for all compounds.

2.2.1.3 Solutions to Be Injected

Solutes of analytes dissolved in mobile phase in concentrations 10^{-4} M to 10^{-3} M to prepare the solutions to be injected. The injection volume was 10 μL. Citric acid solution was used as the unretained compound to determine t_0 in equation (2-1).

For compounds 22-24 and 26-31 in table 3.1, the log k_{wIAM} values were determined directly in the aqueous mobile phase. While for other compounds (lipophilic compounds) a pure aqueous mobile phase was tried but the retention times were too long. Thus, to extrapolate log k values to 100 % water by application of equation (2-2), four or five different methanol concentrations in aqueous solution as mobile phase were used.

$$\log k = \log (t_r - t_0) / t_0 \qquad [2\text{-}1]$$

where t_r and t_0 are the retention times of the solute and of an unretained compound, respectively.

$$\log k = -S\varphi + \log k_{wIAM} \qquad [2\text{-}2]$$

where φ is the volume fraction of methanol in the mobile phase, *S* the slope, and log k_{wIAM} the intercept of the regression curve. For hydrophilic compounds, log k_{wIAM} can be determined directly by using the aqueous mobile phase.

2.2.2 XBridge™ Shield RP_{18} Stationary Phase

2.2.2.1 Determination of Retention Times (t_r)

The retention times were measured with a liquid chromatograph equipped with a HPLC pump SYSTEM GOLD 125 solvent module, a SYSTEM GOLD 507e autosampler and a SYSTEM GOLD UV/Vis 168 detector (all from Beckmann Coulter, INC. Fuerton, CA, U.S.A.). The column used was an XBridge™ Shield RP_{18} (5 cm X 4.6 mm ID, 5µm) from Waters (Milford, MA, U.S.A.).

2.2.2.2 Mobile Phase

The mobile phase comprised 0.02 M phosphate buffer containing methanol in varying proportions from 70 to 10% (v/v). For all non-ionizable compounds, the phosphate buffer was adjusted at pH 7.0. While for ionisable compounds, the buffer was adjusted at a pH value were the neutral form was in large excess for the acidic, ampholytic and basic compounds according to their p*K*a values. A very small amount (0.25% (v/v)) amount of n-octanol was added to methanol and n-octanol saturated water was used to prepare the buffer to increase the simulation with n-octanol/buffer partitioning (*17, 76, 77*). Before addition of methanol containing n-octanol to phosphate buffer, phosphate buffer was filtered under vacuum through a 0.45µm HA Millipore filter (Millipore, Milford, MA, U.S.A.). At room temperature and by using the UV/VIS detector at the specific λ_{max} of the each analyte, the retention times were calculated.

2.2.2.3 Solutions to Be Injected and Flow Rate

The injected samples were prepared by dissolving each solute in an appropriate mobile phase to get the concentration (10^{-4} to 10^{-3} M). The injection volume was 10 µl. Uracil was used as an unretained compound. The measurements were done at a flow rate 1.0 for the compounds with log P_{oct} values higher than 1 and 0.5 ml/min for the compounds with log P_{oct} lower than 1.Three different methanol percents were used to extrapolate to log.K_w According to the log P_{oct} value of the analyte, methanol percentage was chosen as shown in table 2.1. The capacity factor log *K* was calculated by equation (2-1). From the mean of three measurements of *K,* log

K values were obtained. Extrapolation of log *K* to 100 % water condition were done applying equation (2-3).

$$\log K = -S\varphi + \log K_w \qquad [2\text{-}3]$$

where φ is the volume fraction of methanol in the mobile phase, *S* the slope, and log K_w the intercept of the regression curve. For hydrophilic compounds, log K_w can be determined directly by using the aqueous mobile phase.

Table 2.1. Concentrations of Organic Modifier (Methanol) used with XBridge^{TM} Shield RP_{18} Stationary Phase

log P_{oct} of solutes	Methanol % in mobile phase
>3	60,65,70
1-3	30,35,40
<1	10,15,20

2.2.2.4 Linear Solvation Free-Energy Relationships Interpretation

Linear Solvation Free-Energy Relationships (LSERs) concept was developed in (*78-82*). For many chemical systems, there are linear relationships between some properties and the free energy of the reaction, the free energy of transition, or the activation energy, parameters related to the fundamental parameters of the solvents and solutions. According to this concept, chromatographic retention is described by a linear relationship between the log retention time (log *K*) and the parameters that describe the free energy of the reaction. The LSERs can be expressed by equation (2-4):

$$S_p = v \cdot V_w + p\,\pi^* + a\,\alpha + b\,\beta + c \qquad [2\text{-}4]$$

where S_p is a given molecular property of a neutral organic solute (*i.e.*, log K_w or log P_{oct} in the present work). The four structural parameters are the van der Waals volume V_w accounting for hydrophobic and dispersive forces, and polar terms known as solvatochromic parameters (dipolarity/polarizability π^*, H-bond donor acidity α, and H-bond acceptor basicity β) that account for polar interactions between solute and solvents. The regression coefficients *v*, *p*, a, and *b* reflect the relative contribution of each solute parameter to S_p.

So, the compounds carefully selected to have relatively rigid structures and well-defined structural parameters (V_w, π^*, α,*and* β), and covering broad range of structural parameters and

log P_{oct} values (-0.69—5.12) as far as possible so as to establish log K_w/ log P_{oct} relation and LSERs equations.

2.2.3 Temoporfin Transfer between Liposomal Membranes

2.2.3.1 Preparation and Characterisation of Donor and Acceptor Liposomes

Liposome preparation was carried out by a well-established thin-film hydration method. Chloroform solution of lipids and [^{14}C]mTHPC were dried at a temperature at least ten degrees above the gel-to-liquid crystalline phase transition (T_m) of the lipid used by using rotavapor Büchi R 114, (Essen, Germany) with a constant rotating speed 60 rpm and under a vacuum of 200 mbar for 15 minutes, 100 mbar for 15 minutes, and 50 mbar for 60 minutes using vacuum pump Büchi Vacobox B-177 (Essen, Germany) and finally under stream of nitrogen gas (until no chloroform smelled). The temperatures were controlled a water bath Büchi B-481, (Essen, Germany). The dried film was hydrated by trizma buffer saline (pH7.4 and 10 mM). The resulting film was completely dispersed by vortexing for 10 minutes (until complete dispersion of the dried film). The suspension was equilibrated for two hours; this causes the newly formed multilamellar vesicles (MLVs) to be completely hydrated. The resulting liposome suspension was extruded through a polycarbonate membrane filter with pore diameter 100 nm (*83*). The final donor vesicle composition was 70 mol % phospholipid, 10 mol % DCP, 20 mol % of Chol loaded with appropriate amount of [^{14}C-mTHPC]. Acceptor vesicles comprised 80 mol % POPC and 20 mol % of Chol. Particle size analysis and Zeta potential measurements of the vesicles were determined by photon correlation spectroscopy (PCS) using a Zetasizer Nano ZS (Malvern, UK). The samples were diluted with Milli-Q water and measured at 25 C. Liposomes were routinely checked for lamellarity by Cryo-Transmission Electron Microscopy (Cryo-TEM).

2.2.3.2 Preparation of Ion Exchange Gels (DEAE- Sepharose™ CL-6B and CM Sepharose™ Fast Flow)

DEAE Sepharose™ CL-6B and CM Sepharose™ Fast Flow were bought as 20 % ethanolic buffer solution. Appropriate amount of the gel were poured gently in an Erlenmeyer flask avoiding air bubbles formation. The material was left to settle down; afterwards the supernatant was carefully removed by using a Pasteur pipette connected via tubings to a water jet vacuum. The material is washed by three-fold, with trizma buffer saline 10 mM three times, and twice with iso-osmolar sucrose buffer (with NaN_3 0.02 % as preservative). Finally,

the gel was kept in iso-osmolar sucrose buffer (with NaN_3 0.02 %) 1:1. at 4°C (all buffers were adjusted at pH 7.4).

2.2.3.3 Production of Micro-columns

Micro-columns, rubber rings, and sealing are washed with Milli-Q-water. A small volume of glass wool was used as a plug for the column material. Using a Pasteur pipette, approx. 1.0 ml ion exchange suspension was filled in the column. The column is packed with 2 ml of sucrose buffer (40 drops/min). The gel was lipid-saturated by eluting an appropriate amount of acceptor liposomes. Afterwards the column was eluted with 1.5 ml buffer sucrose buffer (with NaN_3 0.02 %).

2.2.3.4 Incubation of Donor and Acceptor Liposomes

In a brown glass vial, donor and acceptor liposome suspensions were mixed. Incubation was carried out in Trizma buffer saline, pH 7.4, at specified temperatures with continuous gentle stirring.

2.2.3.5 Separation of Vesicles and Drug Transfer Measurements

Two populations of vesicles, negatively charged "donor" vesicles and neutral "acceptor" vesicles were separated by charge on ion-exchange columns by a method based on the procedure of Hellings et al. (*84*) as modified by van den Besselaar et al. (*85*). After packing and saturation of micro-columns, the sample applied to surface of the column (allowed to enter the column completely), and eluted with 1.0 ml of the iso-osmolar sucrose buffer. This eluate was collected directly into liquid scintillation vials. Samples were added to Rotiszint® eco plus liquid scintillation cocktail from Roth (Karlsruhe, Germany) and vortexed well for 1 minute. After 24 hours, the samples were analyzed by liquid scintillation counting (LSC) of [^{14}C]mTHPC using Liquid Scintillation Analyzer Tri-Carb 2800TR (PerkinElmer, USA) .

2.2.3.6 Method Validity

In a separate experiment, the recovery of the acceptor vesicles and the retention of the donor vesicles were investigated. Appropriate amount of radiolabeled donor vesicles containing ^{3}H-Cholesteryl-oleate and acceptor vesicles containing ^{14}C-Cholesteryl-oleate which were used as non-exchangeable markers (*35*) and mixture of them applied each to six micro-columns. The eluates were examined by LSC of non-exchangeable markers.

2.2.3.7 Effect of Total Lipid Content on [^{14}C]mTHPC Transfer Kinetics

For the investigation of [^{14}C]mTHPC transfer mechanism regarding the total lipid concentration, the rate of [^{14}C]mTHPC transfer was examined over a wide range of total lipid concentrations at 37 ^{o}C (±1). The donor vesicles (DMPC:Chol:DCP; 7:2:1) concentration was varied over a range 0.1mg, 1mg, and 2mg/ml while acceptor vesicles (POPC:Chol; 8:2) concentration was varied over a range 1mg, 10mg, and 20mg/ml with a constant ratio between donor and acceptor lipid 1:10 mg/mg.

2.2.3.8 Effect of Temperature on [^{14}C]mTHPC Transfer Kinetics

The temperature dependence of [^{14}C]mTHPC transfer kinetics between large unilamellar vesicles at six different temperatures 15, 19, 22, 25, 30, and 37 ^{o}C (±1) was investigated. The activation energy for this process between 15 and 37 ^{o}C was calculated according to the Arrhenius equation. Enthalpy, entropy, and free energy were calculated from Van't Hoff equation. Vesicles were mixed at a concentration of 0.1mg of donor vesicle lipid/ml (DMPC:Chol:DCP; 7:2:1) and 5.0 mg of acceptor vesicle lipid/mL (POPC:Chol; 8:2).

2.2.3.9 Effect of Donor Liposome Charge on [^{14}C]mTHPC Transfer Kinetics

The influence of donor liposome charge on [^{14}C]mTHPC transfer kinetics was investigated by using positively and negatively charged vesicles as donors at 37±1 ^{o}C. Positively charged vesicles comprised (DOPC/DOTAP/Chol; 5:3:2) while negatively charged vesicles were composed of (DOPC/DCP/Chol; 7:1:2). Acceptor vesicle composition was (POPC:Chol; 8:2). Vesicles were mixed at a concentration of 1mg of donor vesicle lipid/ml and 10mg of acceptor vesicle lipid/ml.

2.2.3.10 Effect of Donor Lipid Saturation on [^{14}C]mTHPC Transfer Kinetics

To further evaluate the inner bilayer structure influencing the transfer kinetics of [^{14}C]mTHPC, the sensitivity of transfer to variation in acyl chain saturation was examined. While keeping the phosphocholine head group and chain length constant, the fatty acids for 1,2-diacyl species were varied in terms of degree of saturation. The donor vesicles composition was 70 mol % of (DOPC or SOPC or DSPC), 20 mol % Chol, 10 mol % DCP. Acceptor vesicles comprised 80 mol % POPC and 20 mol % Chol. The donor lipid concentration was 1mg/mL while the acceptor lipid concentration was 10mg/ml and the temperature was kept at 37 ±1 ^{o}C.

2.2.3.11 Effect of Acyl Chain Length of Donor Vesicles on [^{14}C]mTHPC Transfer Kinetics

This experiment was an extension to the above one in order to investigate the influence of acyl chain length (rigidity) of donor liposomes on transfer [^{14}C]mTHPC between liposomal membranes. The phosphocholine head groups of saturated fatty acids were kept the same while the 1,2-diacyl species were varied in terms of acyl chain length. The donor vesicles composition was 70 mol % of [DMPC (14:0/14:0) or DPPC (16:0/16:0) or DSPC (18:0/18:0) or DBHPC (22:0/22:0)], 20 mol % Chol, 10 mol % DCP. Acceptor vesicles comprised 80 mol % POPC and 20 mol % Chol. The donor lipid concentration was 1mg/ml while the acceptor lipid concentration was 10mg/ml at a temperature of 37 ±1 ^{o}C.

2.2.3.12 Calculations

The transfer curves of the percentage [^{14}C]mTHPC transferred were exponentially fitted using Microcal Origin 6.0 software (OriginLab Corporation, US-Northampton) and the exponential function:

$$y = y_{\infty}\left(1 - e^{-k(t-t_0)}\right). \qquad \textbf{[2-6]}$$

Here, y is the percentage of [^{14}C]mTHPC transferred to the acceptor vesicles at time t, and y_{∞} denotes the final percentage of [^{14}C]mTHPC transferred, corresponding to the height of the plateau. Conducting the experiments involves a small time offset t_0 that is incorporated in equation (2-6). The constant K is the apparent rate constant of the transfer.

In the Appendix, equation (5-1) driven from a simple kinetic transfer model that accounts for two different transfer mechanisms, collisions between liposomes (characterized by a rate constant K_c) and diffusion of [^{14}C]mTHPC through water (characterized by a rate constant K_d). The apparent rate constant is then $K = K_d + c\ K_c$ where c is the total concentration of liposomes (both donor and acceptor) in the aqueous solution. The dependence of the measured rate constants K on the concentration of donor and acceptor liposomes suggests the transfer mechanism to be either diffusion or collision controlled.

Half lifes were calculated from K as

$$t_{1/2} = \ln 2 / K \qquad \textbf{[2-7]}$$

The apparent transfer coefficient ($K_{D\rightarrow A}$) of [^{14}C]mTHPC between donor vesicles and acceptor vesicles was calculated from the following equation (2-8):

$$K_{D\rightarrow A} = \frac{C_A}{C_D} \qquad \textbf{[2-8]}$$

where, C_A is the amount of [^{14}C]mTHPC in the acceptor vesicles at equilibrium and C_D is the amount of [^{14}C]mTHPC in the donor vesicles at equilibrium at certain temperature.

The temperature dependence of the equilibrium transfer coefficient is given from Van't Hoff plot of $Ln\ K_{D\rightarrow A}$ versus T^{-1}

$$LnK_{D\rightarrow A} = \frac{-\Delta H}{RT} + \frac{\Delta S}{R} \qquad \textbf{[2-9]}$$

were, $-\Delta H/R$ refers to the slope of the line and $\Delta S/R$ is the intercept. ΔH ($KJ\ mol^{-1}$) is the enthalpy of the transfer, ΔS ($J\ mol^{-1}\ K^{-1}$) is the entropy of the transfer, T is the absolute temperature, and R is the gas constant (8.31 $J\ mol^{-1}\ K^{-1}$).
Once ΔH and ΔS are known from the former correlation, the free energy ΔG of the transfer can be calculated from the expression:

$$\boldsymbol{\Delta G = \Delta H - T\Delta S} \qquad \textbf{[2-10]}$$

N.B. All regression analyses were performed via the Microcal Origin statistical software package version 6.0 (Microcal Origin software Inc, Northapton, MA, USA).

PART III
RESULTS AND DISCUSSION

3. RESULTS AND DISCUSSION

Drugs, whether in formulations which contain more than one phase or in the body, move from one liquid phase to another in ways that depend on their relative concentrations (or chemical potentials) and their affinities for each phase. So, a drug will move from the blood into extravascular tissues if it has the appropriate affinity for the cell membrane and the non-blood phase. The movement of molecules from one phase to another is called partitioning. In this work, two different artificial membranes, immobilized artificial membrane (IAM.PC.DD2) and XBridge^{TM} shield RP_{18} stationary phase have been used to study the partitioning of some of chemical compounds between the aqueous phase and the non-blood phase. In addition, the drug transfer between liposomal drug delivery system and liposomal artificial membrane has been studied.

3.1 Immobilized Artificial Membrane (IAM.PC.DD2)

A set of monofunctional compounds and complex drugs (steroids, non-steroidal anti-inflammatory drugs, and β-blockers) have been tested to understand the retention mechanism of solutes on an IAM stationary phase. This set includes neutral solutes and solutes with acidic or basic functionalities which are positively charged or negatively charged at pH 7.0, as shown in table 3.1. The influence of different functionalities, lipophilicity, and the charged state of the solutes was investigated with respect to retention behaviour of different sets of analytes.

In this part of work, the obtained values of the capacity factors (log k_{wIAM}) were compared with the n-octanol/water partitioning values (log P_{oct}). For the ionized compounds, the electrostatic interaction with phospholipids was found.

To simulate the physiologic pH regarding the stationary phase stability (highest pH limit is 7.5), retention times were measured at pH 7.0 on the IAM.PC.DD2 stationary phase. The monofunctional carboxylic acids (22 – 30) and the NSAIDs (31 – 36) are fully negatively charged at pH 7.0 according to the pK_a values of the compounds shown in table 3.1, whereas basic compounds including (4-methylbenzyl) alkylamines (37 – 43) and β-blockers (44 – 49) are fully positively charged. For the very weak bases and acids (1 – 5, 12, and 13), a neutral form at this pH was found. The pK_a values, charge state of the compounds, the partition coefficient (log P_{oct}), and distribution coefficient at pH 7.0, namely log $D_{7.0}$ calculated from pK_a and log P_{oct} values, are shown in table 3.1.

3.1.1 Relationship between log *k* and φ

A pure aqueous mobile phase was used to elute the analytes 22 – 24 and 26 – 31, whereas for the other compounds, four or five different methanol concentrations were added to the aqueous mobile phase for the extrapolation to log k_{wIAM} values. Considering the range of the eluent composition studied, good linear relationships between log *k* and φ were attained. The squared correlation coefficient was higher than 0.99, except for the log k_{wIAM} of compounds numbers 3, 4, 10, and 46 in table 3.1 (R^2=0.98). The log k_{wIAM} values are presented in table 3.1 together with other physicochemical parameters.

Table 3.1. The physicochemical parameters of the investigated solutes

	Compounds	Log P_{oct} [a)]	pK_a [a)]	log $D_{7.0}$ [b)]	charge state	log k_{wIAM} [c)]
1	Acridine	3.40	5.58	3.40	N	2.42
2	$C_6H_5NH_2$	0.90	4.60	0.90	N	0.26
3	$C_6H_5NHC_2H_5$	2.16	5.12	2.16	N	1.04
4	2-Cl-$C_6H_4NH_2$	1.91	2.64	1.91	N	1.14
5	2-NH_2-C_6H_4-C_6H_5	2.84	3.82	2.84	N	2.02
6	$C_6H_5CH_2CN$	1.56	N	1.56	N	0.94
7	C_6H_5-CO-CH_3	1.58	N	1.58	N	0.86
8	$C_6H_5NO_2$	1.85	N	1.85	N	0.99
9	2-$ClC_6H_4NO_2$	2.24	N	2.24	N	1.58
10	$C_6H_5CH_2OH$	1.08	N	1.08	N	0.58
11	4-Cl-$C_6H_4CH_2OH$	1.96	N	1.96	N	1.21
12	3-Cl-C_6H_4OH	2.49	9.11	2.48	N	1.77
13	3-NO_2-C_6H_4-OH	2.00	8.40	1.96	N	1.38
14	Corticosterone	1.94	N	1.94	N	1.67
15	Dexamethasone	1.83	N	1.83	N	1.79
16	Estradiol	4.01	N	4.01	N	2.65
17	Estrone	3.13	N	3.13	N	1.92
18	Hydrocortisone	1.55	N	1.55	N	1,35
19	Hydrocortisone-21-acetate	2.19	N	2.19	N	1.78
20	Progestrone	3.87	N	3.87	N	3.01
21	Testosterone	3.29	N	3.29	N	2.51
22	$C_6H_5(CH_2)_2COOH$	1.89	4.52	-0.59	-	-0.25
23	$C_6H_5(CH_2)_3COOH$	2.42	4.72	0.14	-	0.06
24	$C_6H_5(CH_2)_4COOH$	2.85	4.55	0.40	-	0.43
25	$C_6H_5(CH_2)_7COOH$	4.09	5.03	2.12	-	2.02
26	C_6H_5COOH	1.96	4.20	-0.84	-	-0.62
27	4-BrC_6H_4COOH	2.86	3.97	-0.17	-	0.32

28	3-ClC_6H_4COOH	2.71	3.83	-0.46	-	0.06
29	4-IC_6H_4COOH	3.13	3.96	0,09	-	0.51
30	1-Naphthoic acid	3.10	3.69	-0.21	-	0.13
31	Aspirin	1.13	3.48	-2.39	-	-0.15
32	Flurbiprofen	3.81	3.91	0.72	-	1.78
33	Ketoprofen	2.77	4.29	0.06	-	1.26
34	Naproxen	3.06	4.15	0.21	-	1.35
35	Indomethacin	4.27	4.50	1.77	-	2.37
36	Mefenamic acid	5.12	4.33	2.45	-	2.35
37	4-$CH_3C_6H_4CH_2NHCH_3$	1.96	9.93	-0.97	+	0.96
38	4-$CH_3C_6H_4CH_2NHC_2H_5$	2.38	10.04	-0.66	+	1.02
39	4-$CH_3C_6H_4CH_2NHC_3H_7$	2.96	9.98	-0.02	+	1.30
40	4-$CH_3C_6H_4CH_2NHC_4H_9$	3.49	9.98	0.51	+	1.87
41	4-$CH_3C_6H_4CH_2NHC_5H_9$	4.26	10.08	1.18	+	2.27
42	4-$CH_3C_6H_4CH_2NHC_6H_{11}$	4.96	10.17	1.79	+	2.77
43	4-$CH_3C_6H_4CH_2NHC_7H_{13}$	5.12	10.02	2.10	+	2.92
44	Metoprolol	1.95	9.63	-0.68	+	1.45
45	Metipranolol	2.81	9.54	0.27	+	1.78
46	Oxprenolol	2.51	9.57	-0.06	+	1.70
47	Penbutolol	4.62	9.92	1.70	+	3.70
48	Pindolol	1.75	9.54	-0.79	+	1.31
49	Propranolol	3.48	9.53	0.95	+	2.48

[a]) Taken from references (*86-89*). [b]) Calculated according to $\log D_{7.0} = \log P_{oct} - \log (1 + 10^{pKa - pH})$ for bases and $\log D_{7.0} = \log P_{oct} - \log (1 + 10^{pH - pka})$ for acids. [c]) n = 3, s.d. ≤ 0.05. N = Neutral

3.1.2 Relationship between log k_{wIAM} and log P_{oct}

No correlation was found for all compounds under investigation in one equation. However, good correlations for neutral compounds or structurally related compounds were found. The resulting equations for the relation between log k_{wIAM} and log P_{oct} are shown as follows below in equations 3-1 – 3-5. In these equations, 95% confidence limits are in parentheses, *n* is the number of compounds, R^2 the squared correlation coefficient, *s* the standard deviation, and *F* Fisher's test. Figure 3.1 shows correlation between log k_{wIAM} and log P_{oct}.

3.1.2.1 Relationship between log k_{wIAM} and log P_{oct} for the neutral compounds

For the neutral molecules (1-21 in table 3.1), reasonable correlation was obtained when all neutral molecules are treated as a one set ($R^2 = 0.87$). While by removing the steroids (14-21) from this list, quite good relationship was established for the 13 mono-functional molecules

(1-13) (R^2=0.95). This result indicates that the correlation significance for neutral solutes is increased by decreasing the structural diversity of the compounds.

log k_{wIAM} = 0.77 (±0.13) log P_{oct} – 0.19 (±0.33) **[3-1]**

n=21, R^2=0.87, s=0.26, F=130

3.1.2.2 Relationship between log k_{wIAM} and log P_{oct} for the β-blockers

In terms of the β-blockers analytes (44-49 in table 3.1), equation 3-2 and figure 3.1 show that the correlation line is identical to that one of the neutral compounds. Barbato and co-workers reported the same results when ten β-blockers on three different types of IAM columns (*90*) were investigated. This result indicates that although the β-blockers compounds are completely ionized bearing positive charges under the experimental conditions, they can interact strongly with phospholipids like neutral compounds with the same log P_{oct} values. This means that rather than lipophilicity, the retention behaviour of the β-blockers under study on IAM:PC:DD2 stationary phase is controlled by electrostatic interaction between positively charged amines of β-blockers and negatively charged phosphates of phospholipids as mentioned by Avdeef et al. (*91*) and Barbato et al. (*90, 92*).

log k_{wIAM} = 0.84 (±0.16) log P_{oct} – 0.34 (±0.48) **[3-2]**

n=6, R^2=0.97, s=0.18, F=115

3.1.2.3 Relationship between log k_{wIAM} and log P_{oct} for the 4-methylbenzyl alkylamines

Although these substances are positively charged under these experimental conditions like β-blockers, the interaction of the seven positively charged (4-methylbenzyl) alkylamines (37 – 43 in table 3.1) with the phospholipids on IAM.PC.DD2 stationary phase was weaker than that of the β-blockers and neutral compounds having the same log P_{oct} values. This phenomenon means that the strength of the electrostatic interaction between charged amines and phospholipids membrane depends on the whole chemical structure of the molecule. These results can be seen from equation 3-3 and figure 3.1.

log k_{wIAM} = 0.65 (±0.07) log P_{oct} – 0.46 (±0.27) **[3-3]**

n=7, R^2=0.98, s=0.11, F=320

3.1.2.4 Relationship between log k_{wIAM} and log P_{oct} for the NSAIDs

It is clear from figure 3.1 and equation 3-4 that the negatively charged NSAIDs (31-36 in table 3.1) under investigation were retained on IAM:PC:DD2 stationary phase less than the positively charged compounds. This result is in contrast with the result from the study of Barbato et al. on IAM.PC.MG stationary phase (*93*). Barbato and co-workers found that the correlation between log k_{wIAM} and log P_{oct} for NSAIDs (with carboxylic function not directly linked to the aromatic ring) and neutral compounds resulted in a good regression line. Whereas, in this study (on IAM.PC.DD2 stationary phase) showed two different regression lines for NSAIDs and neutral compounds. This indicates that the interaction of NSAIDs under investigation is weaker than that of neutral compounds having the same log P_{oct} values on IAM.PC.DD2 stationary phase. Moreover, it could be seen that the regression lines of negatively charged NSAIDs, especially 32-35 in table 3.1, and the positively charged (4-methylbenzyl) alkylamines are identical.

$$\log k_{wIAM} = 0.66\ (\pm 0.16) \log P_{oct} - 0.72\ (\pm 0.55) \qquad [3\text{-}4]$$

n=6, R^2=0.95, s=0.24, F=73

3.1.2.5 Relationship between log k_{wIAM} and log P_{oct} for the monofunctional carboxylic acids

With the exception of 8-Phenyloctanoic acid (25 in table 3.1), the retention of monofunctional carboxylic acids (22 – 30) which are negatively charged at pH 7.0 were also less than the retention of neutral compounds like the negatively charged NSAIDs behaviour on IAM.PC.DD2 stationary phase column. Moreover, although the mono-functional carboxylic acids (22 – 30) are negatively charged at pH 7.0, they showed less retention time than the negatively charged NSAIDs on IAM.PC.DD2 stationary phase column. This difference in retention behaviour could bee seen from different regression lines between log k_{wIAM} and log P_{oct} in figure 3.1. Also it is clear that the correlation coefficient of equation 3-5 is less significant (R^2=0.86), indicating that the retention behaviour of group of molecules can not be well known by their log P_{oct} values. In terms of the molecule 8-phenyloctanoic acid (25 in table 3.1), although it bears a negative charge, it showed a retention behaviour more than all of mono-functional carboxylic acids mimicking the retention behaviour of NSAIDs. This may be ascribed to the fact, that as the chain length of nonpolar aliphatic compounds increases, the partition coefficient (*P*) increases by factor of 2-4 per each methylene group (*94*). Consistently with this fact, 8-Phenyloctanoic acid is more lipophilic than the other mono-

functional carboxylic acids because it has $(-CH_2-)_7$ groups. Owing to the hydrocarbon chain, it displays a high affinity to the phospholipids in IAM.PC.DD2 stationary phase more than the affinity to the aqueous mobile phase.

$$\log k_{wIAM} = 1.02\ (\pm 0.31) \log P_{oct} - 2.54\ (\pm 0.89) \qquad [3\text{-}5]$$

n=9, R^2=0.86, s= 0.29, F=43

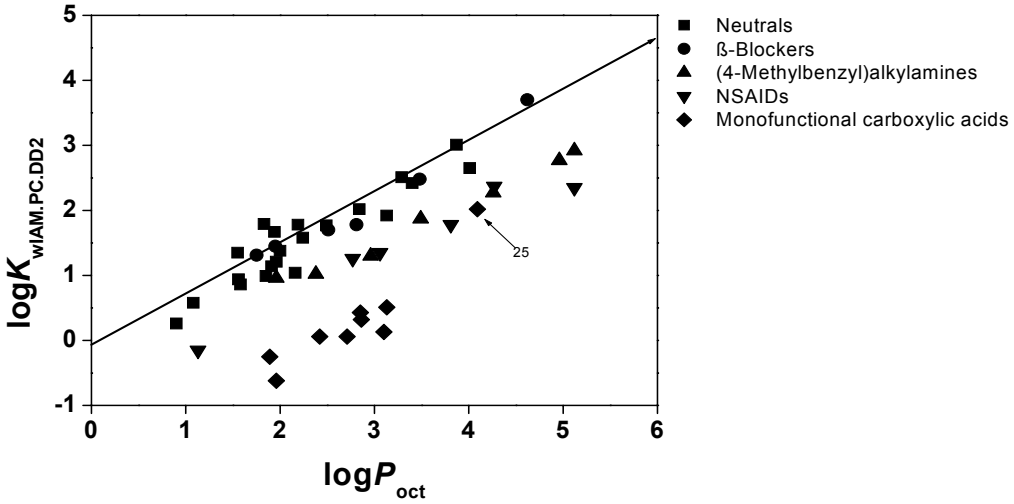

Figure 3.1. The correlation between log k_{wIAM} values from IAM.PC.DD2 stationary phase at pH 7 and log P_{oct} values for the compounds investigated.

3.1.3 Relationship between log k_{wIAM} and log $D_{7.0}$ on IAM.PC.DD2 Column

In terms of NSAIDs and (4-methylbenzyl) alkylamines dealt in this study, the n-octanol/water partition coefficient (a ratio of concentrations of un-ionized compound between the two solutions) and n-octanol/water distribution coefficient (the ratio of the sum of the concentrations of ionized plus un-ionized forms of the compound in the two solutions) values are highly interrelated. As a result, the correlation between the retention behaviour on IAM.PC.DD2 stationary phase (log k_{wIAM}) and the n-octanol/water distribution coefficient (log $D_{7.0}$) was not dealt here any longer. While for β-blockers, the significance of the correlation between log k_{wIAM} and log $D_{7.0}$ values decreased in comparison to that between log k_{wIAM} and log P_{oct}. In contrast, a high significant correlation equation is found out between log k_{wIAM} and log $D_{7.0}$ values for the monofunctional carboxylic acids. This difference in significance can be noted from the comparison between the correlation coefficients of equation 3-5 and equation 3-6. This notion means that the n-octanol/water distribution

coefficient (log $D_{7.0}$) values can be a good interpretation for the retention behaviour of this set of molecules on IAM.PC.DD2 stationary phase.

log k_{wIAM} = 0.82 (±0.16) log $D_{7.0}$+ 0.25 (±0.13) **[3-6]**

n=9, R^2=0.94, s=0.19, F=107

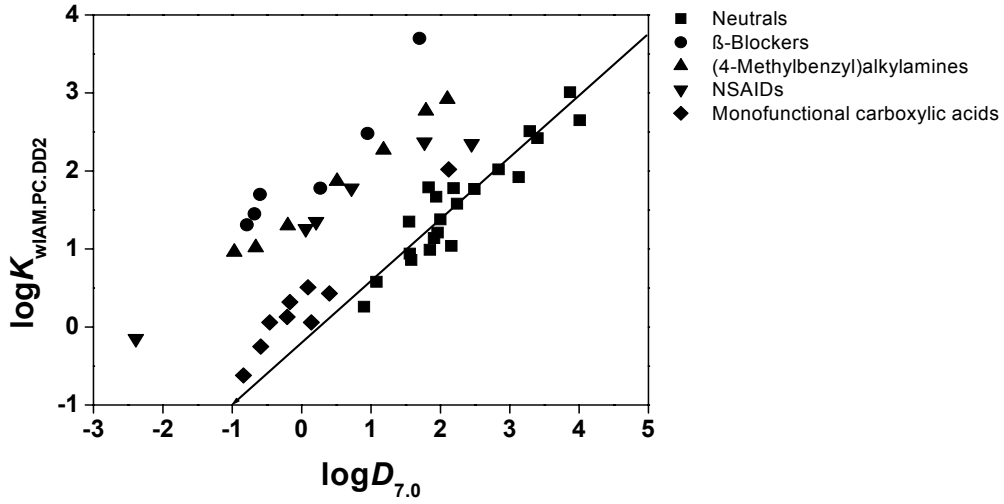

Figure 3. 2. The correlation between log k_{wIAM} values from IAM.PC.DD2 stationary phase at pH 7 and log $D_{7.0}$ values for the compounds investigated.

To elucidate the extra interaction between the charged molecules and the phospholipids of IAM.PC.DD2, the correlation between log k_{wIAM} and the distribution coefficient log $D_{7.0}$ of the compounds under study was established in figure 3.2. The non-ionised compounds showed the least retention on IAM.PC.DD2 stationary phase as can be seen from figure 3.2. In another words, the ionized molecules showed stronger retention behaviour than the neutral compounds with the same log $D_{7.0}$ values, to a different degree, depending on their charge type and structural characteristics. With respect to the charged solutes, the positively charged molecules are more strongly retained than the negatively charged one. As explained by Avdeef et al. for the liposomal membrane/water partitioning of ionized drugs (*91*), the charge distribution in the phospholipid membrane is anisotropic; as the ionized species moves in the direction of the aqueous exterior of the membrane; the first charges it experiences are those of the negatively charged phosphates. Further movement would bring the ionized drug substance in the vicinity of the positively charged trimethyl ammonium groups. Electrostatic pairing of charges would need a greater movement for weak acids, compared to weak bases. Therefore,

the negatively charged solutes have lesser affinity for phosphatidylcholine-based membranes than positively charged solutes. The results from this study with the IAM.PC.DD2 stationary phase verified this point. In addition, the structural characteristics influence also in the retention behaviour of the ionized solutes which bearing the same charge on the IAM.PC.DD2 phase. For instance, β-blockers are slightly more retained than (4-methylbenzyl) alkylamines, which is also stated by Bertschinger et al. in their study (*87*). Also for the negatively charged solutes, monofunctional carboxylic acids are less retained than NSAIDs (except mefenamic acid (36) in table 3.1), verifying the influence of the structural characteristics of the solutes on the electrostatic interaction.

3.2 XBridge^{TM} Shield RP_{18} Stationary Phase

The two most popular HPLC phase, C_{18} and C_8, are the workhorses of liquid chromatography method development. Useful for a wide variety of separations, these columns are familiar to all separation scientists. XBridge C_{18} and C_8 offer methods development flexibility. By employing trifunctional bonding and advanced endcapping, excellent reproducibility, performance, and column lifetime across the entire pH range (1-12) is observed. In recent times, a novel RP-HPLC column (XBridge^{TM} Shield RP_{18}) produced by organic/inorganic Hybrid Particle Technology has become available. The patented Shield Technology incorporates a carbamate group embedded into the bonded phase that "shields" surface silanols. Additionally, it functionally enables compatibility with fully aqueous mobile phases without risk of pore dewetting, resulting in reliable and robust retention. Since the column shows a wide pH resistance (1—12), it is expected to measure with this column lipophilicity also for basic molecules like for neutral and acidic ones.

3.2.1 Selection of the Compounds to Be Examined

A highly informative interpretation from the retention of solutes on RP-HPLC stationary phases can be attained by linear solvation free-energy relationships (LSERs). Also the relationships have been applied in estimation of partitioning mechanisms of molecules in different organic/aqueous biphasic systems (*80-82*). The LSERs can be expressed by equation 3-7.

$$S_p = v \cdot V_w + p\,\pi^* + a\,\alpha + b\,\beta + c \qquad [3\text{-}7]$$

where S_p is a given molecular property of a neutral organic solute (*i.e.*, log K_w or log P_{oct} in the present work). The four structural parameters are the van der Waals volume V_w accounting

for hydrophobic and dispersive forces, and polar terms known as solvatochromic parameters (dipolarity/polarizability π^*, H-bond donor acidity α, and H-bond acceptor basicity β) that account for polar interactions between solute and solvents. The regression coefficients *v*, *p*, *a,* and *b* reflect the relative contribution of each solute parameter to S_p. In the present study, relatively rigid structures and well-known structural parameters (V_w, π^*, α, *and* β) molecules are carefully chosen to be investigated. These solutes cover a broad range of structural parameters and log P_{oct} values (-0.69—5.12) as far as possible so as to establish log K_w /log P_{oct} relation and LSERs equations. The parameters were written in table 3.2. Figure 3.3 shows that the values of parameters for the selected compounds were distributed in a wide range.

3.2.2 Relationship between log *K* and φ

Excluding nitrobenzene and ketoprofen (15 and 32 in table 3.2) (R^2=0.96) and 4-methylbenzyl), ethylamine and 5-phenylvaleric acid (7 and 24 in table 3.2) (R=0.97), the squared correlation coefficient (R^2) was higher than 0.99 for all compounds. This means, an excellent linear relationship between log *K* and φ was found for majority of the compounds tested on the XBridge™ Shield RP_{18} stationary phase. The rightmost column in table 3.2 includes the log K_w values of the molecules for this stationary phase.

3.2.3 Correlation between log P_{oct} and log K_w

The correlation between log P_{oct} and log K_w values on the XBridge™ Shield RP_{18} stationary phase for the 40 compounds can be seen from equation 3-8 and figure 3.4.

$\log P_{oct} = 1.03\ (\pm 0.07) \log K_w + 0.48\ (\pm 0.15)$ **[3-8]**

n=40, q^2=0.96, R^2=0.96, s=0.26, F=968

where the values in the parentheses are the 95% confidence limits; *n*, q^2, R^2, *s* and *F* are the number of compounds, the cross-validated correlation coefficient, the squared correlation coefficient, and the standard deviation and Fisher's test, respectively.

It can be noted from the results that for the whole set of neutral, acidic, ampholytic, and basic compounds, the log K_w values obtained from the XBridge™ Shield RP_{18} phase are significantly well correlated with the log P_{oct} values although the log K_w values are not the same as the log P_{oct} values as indicated by the intercept (+0.48) of equation 3-8. This means that the determination of n-octanol/water partition coefficient by fast and reliable RP-HPLC with XBridge™ Shield RP_{18} column along a wide pH range (1-12) is possible.

The slope of equation 3-8 which almost equal to unity means a significant correlation between log P_{oct} and log K_w on the XBridge^{TM} Shield RP_{18} phase. This result is good correlation between the partitioning process in n-octanol/water and the chromatographic retention process on this stationary phase (*17*). One can speculate, that this similarity is originating from the amido groups embedded in the stationary phase. The silica-based Discovery-RP-Amide-C16 phase produced also a significant correlation between log P_{oct} and log K_w for neutral and acidic drugs. This may be also ascribed to that it has the same amido groups as the XBridge^{TM} Shield RP_{18} phase (*17, 77*). A highly significant correlation between the log K_w values obtained with two stationary phases, silica-based Discovery-RP-Amide-C16 phase and XBridge^{TM} Shield RP_{18} phase, for the 32 common solutes presented in equation 3-9 and figure 3.5. This result confirm that the polar amido groups embedded in the alkyl chains of the two stationary phases are main the reason to yield a good correlation between log K_w values and log P_{oct} values.

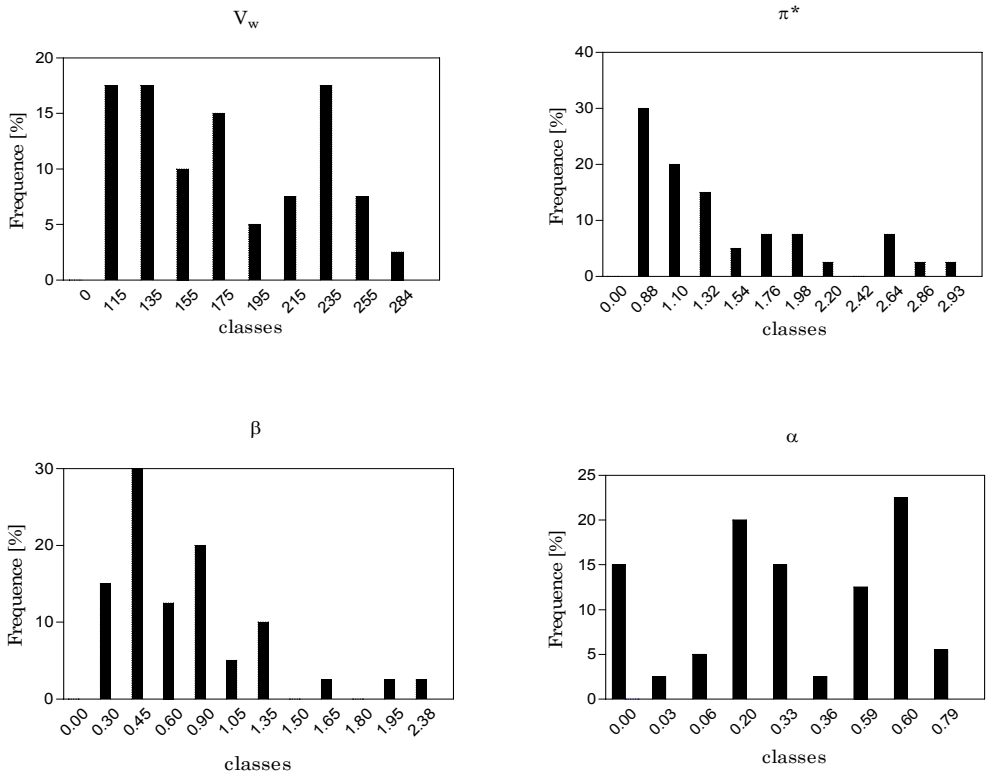

Figure 3.3. Distribution of the 40 investigated compounds (table 3.2) in the parameter spaces of van der Waals volume V_w, dipolarity/polariability π^*, H-bond acceptor basicity β and H-bond donor acidity α.

Table 3.2. Investigated compounds and their physicochemical parameters

No.	Solutes	V_w [a,b]	π^* [a,c]	β [a,d]	α [a,e]	log P_{oct} [a]	pK_a [f]	log K_w [g] on XBridge™ Shield RP_{18}
	Model solutes							
	Bases							
1	Acridine	174.9	1.57	0.52	0.00	3.40	5.58	2.42
2	$C_6H_5NH_2$	98.0	0.94	0.41	0.06	0.90	4.60	0.70
3	$C_6H_5NHC_2H_5$	133.0	0.78	0.45	0.03	2.16	5.12	1.48
4	2-Cl-$C_6H_4NH_2$	111.8	1.06	0.41	0.06	1.91	2.64	1.30
5	2-NH_2-C_6H_4-C_6H_5	173.9	1.55	0.41	0.18	2.84	3.82	2.26
6	4-$CH_3C_6H_4CH_2NHCH_3$	149.5	0.80	0.70	0.08	1.96	9.93	1.10
7	4-$CH_3C_6H_4CH_2NHC_2H_5$	166.1	0.80	0.70	0.08	2.38	10.04	1.35
8	4-$CH_3C_6H_4CH_2NHC_3H_7$	183.4	0.80	0.70	0.08	2.96	9.98	1.75
9	4-$CH_3C_6H_4CH_2NHC_4H_9$	199.4	0.80	0.70	0.08	3.49	9.98	3.15
10	4-$CH_3C_6H_4CH_2NHC_5H_9$	217.7	0.80	0.70	0.08	4.26	10.08	3.75
11	4-$CH_3C_6H_4CH_2NHC_6H_{11}$	234.2	0.80	0.70	0.08	4.96	10.17	4.36
12	4-$CH_3C_6H_4CH_2NHC_7H_{13}$	251.8	0.80	0.70	0.08	5.12	10.02	4.96
	Neutrals							
13	$C_6H_5CH_2CN$	121.5	1.22	0.45	0.00	1.56		1.24
14	C_6H_5-CO-CH_3	122.3	1.12	0.51	0.00	1.58		1.08
15	$C_6H_5NO_2$	107.6	1.01	0.28	0.00	1.85		1.36
16	2-$ClC_6H_4NO_2$	122.0	1.13	0.28	0.00	2.24		1.93
17	$C_6H_5(CH_2)_2C_6H_5$	196.9	0.99	0.20	0.00	4.80		4.00
18	$C_6H_5CH_2OH$	111.6	0.84	0.58	033	1.08		0.65
19	4-Cl-$C_6H_4CH_2OH$	126.3	0.96	0.58	0.33	1.96		1.39
	Acids							
20	3-Cl-C_6H_4OH	107.8	0.84	0.16	0.69	2.49	9.11	2.08
21	3-NO_2-C_6H_4-OH	112.9	1.54	0.23	0.79	2.00	8.40	1.53
22	$C_6H_5(CH_2)_2COOH$	146.0	1.12	0.45	0.60	1.89	4.52	1.27
23	$C_6H_5(CH_2)_3COOH$	162.4	1.12	0.45	0.60	2.42	4.72	1.75
24	$C_6H_5(CH_2)_4COOH$	179.8	1.12	0.45	0.60	2.85	4.59	2.20
25	C_6H_5COOH	111.8	0.74	0.40	0.59	1.96	4.20	1.31
26	4-BrC_6H_4COOH	133.8	0.94	0.40	0.59	2.86	3.97	2.31
27	3-ClC_6H_4COOH	126.2	0.86	0.30	0.59	2.71	3.83	2.17
28	4-IC_6H_4COOH	141.6	0.96	0.42	0.59	3.13	3.96	2.53
29	1-Naphthoic acid	158.5	1.05	0.40	0.59	3.10	3.69	2.52
	Drugs							
30	Flurbiprofen	223.1	1.78	0.49	0.60	3.81	3.91	3.62
31	Indomethacin	283.5	1.86	1.29	0.60	4.27	4.50	3.76
32	Ketoprofen	239.1	2.12	0.99	0.60	2.77	4.29	2.18

33	Naproxen	216.5	1.64	0.79	0.60	3.06	4.15	2.24
34	Phenytoin	228.3	1.45	1.02	0.60	2.68	8.33	1.57
35	Sulfabenzamide	233.6	2.48	1.25	0.33	1.46	1.70/ 4.57	1.09
36	Sulfacetamide	174.8	2.58	1.25	0.33	-0.16	1.78/ 5.28	-0.51
37	Sulfamethazine	237.5	2.72	1.90	0.33	0.25	2.73/ 7.52	0.01
38	Sulfamethoxazole	207.5	2.59	1.64	0.36	0.72	2.28/ 5.68	0.60
39	Sulfamethoxypyridazine	229.6	2.93	2.38	0.33	0.35	2.09/ 7.02	0.17
40	Sulfanilamide	139.1	1.89	1.26	0.60	-0.69	2.15/ 10.42	-0.87

a) Taken from reference (*95*). b) Van der Waals volume. c) Dipolarity/polarizability. d) H-bond acceptor basicity. e) H-bond donor acidity. f) Taken from references (*86, 87, 96*). g) $0.01 \leq S.D \leq -0.15$.

Table 3.3. Compounds in the Test Set

	Solutes	**log P_{oct} [a)]**	**pK_a [b)]**	**log K_w [c)] on XBridge^{TM} Shield RP_{18}**	**log P [d)]**
41	Antipyrine	0.17	-0.04	-0.04	0.44
42	Aspirin	1.19	0.40	0.40	0.89
43	Estradiol	4.01	3.36	3.36	3.94
44	Hydrocortisone	1.55	0.81	0.81	1.31
45	Mefenamic acid	5.12	4.34	4.34	4.95
46	Metoprolol	1.95	1.00	1.00	1.51
47	Penbutolol	4.62	4.06	4.06	4.66
48	Phenylbutazone	3.16	2.35	2.35	2.90
49	Pindolol	1.75	9.54	0.71	1.21
50	Progestrone	3.57	3.37	3.37	3.95
51	Promethazine	4.81	4.08	4.08	4.68
52	Propranolol	3.48	2.78	2.78	3.34
53	Testosterone	3.32	268	2.68	3.24

[a]) Taken from (*17, 87*). [b]) Taken from (*86*). [c]) $0.01 \leq SD \leq 0.15$ [d]) Partition coefficient predicted by equation 10.

$$\log K_{w\ (XBridgeTM\ Shield\ RP18)} = 1.03\ (\pm 0.06) \log K_{w\ (Discovery\ RP\ Amide\ C16)} + 0.17\ (\pm 0.12) \qquad \textbf{[3-9]}$$

$n=32$, $q^2=0.9$, $R^2=0.97$, $s=0.20$, $F=926$

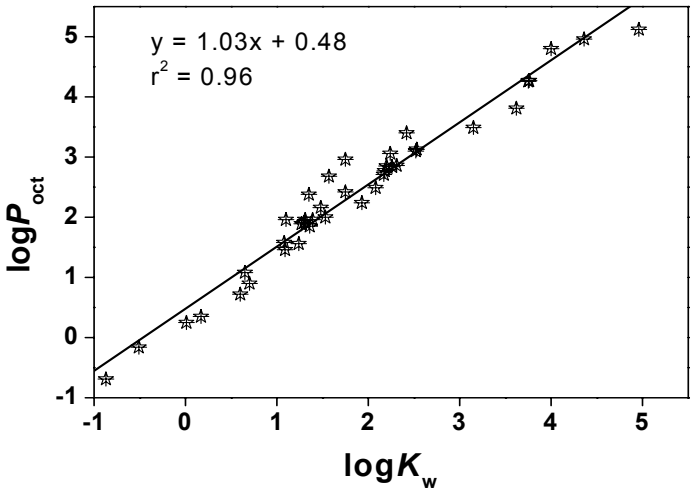

Figure 3.4. Relationship between log P_{oct} and log K_w obtained with the XBridge™ Shield RP_{18} stationary phase.

To judge, if the capacity factor (log K_w) resulted from the XBridge™ Shield RP_{18} can predict lipophilicity (log P_{oct}), a group of 13 molecules listed in table 3.3 with a wide structural diversity and known log P_{oct} values were investigated to found the predictive power of equation 3-8. The rightmost column and the second rightmost column in table 3.3 contain the log K_w values from the XBridge™ Shield RP_{18} phase and the log P_{oct} values predicted by equation 3.8. It can be seen from these new values predicted by equation 3.8 that the lipophilicity index log K_w gives an acceptable evaluation of log P_{oct} as shown in equation 3-10. This is considered a successful application of the XBridge™ Shield RP_{18} stationary phase in log P_{oct} prediction under the present experimental conditions.

$$\log P_{oct} = 0.94\ (\pm 0.09)\ \log P_{(\text{est. from log } Kw)} + 0.27\ (\pm 0.30) \qquad [3\text{-}10]$$

n=13, q^2=0.98, R^2=0.98, s=0.25, F=429

Since the XBridge™ Shield RP_{18} phase can give log K_w values highly correlated with log P_{oct} values for all types of compounds, acidic, basic, and neutral with a wide range of log P_{oct}, it can be concluded that XBridge™ Shield RP_{18} stationary phase can be used instead of the shake-flask method in determination of lipophilicity.

3.2.4 Comparison by LSERs Analysis between the Retention Mechanism on the XBridge™ Shield RP_{18} Phase and the Partitioning Mechanism in n-octanol/water

For the 40 analytes with known solvatochromic parameters listed in table 3.2, the log K_w values obtained with the XBridge™ Shield RP_{18} stationary phase were analyzed using linear solvation free-energy relationships (LSERs). The structural properties governing retention mechanism on XBridge™ Shield RP_{18} stationary phase were described by obtained statistically significant equations 3-11 and 3-11a.

$$\textbf{Log } K_w = 2.61\cdot10^{-2}\ (\pm0.41\cdot10^{-2})\ V_w - 0.64\ (\pm0.48)\ \pi^* - 2.00\ (\pm0.66)\ \beta - 0.09\ (\pm0.65)\ \alpha - 0.32\ (\pm0.65) \quad \textbf{[3-11]}$$

n=40, q^2=0.84, R^2=0.85, s=0.51, F=52

After the removal of the non-significant variable **α**,

$$\textbf{log } K_w = 2.61\ 10^{-2}\ (\pm0.41\cdot10^{-2})\ V_w - 0.66\ (\pm0.45)\ \pi^* - 1.98(\pm0.64)\ \beta - 0.33\ (\pm\ 0.64) \quad \textbf{[3-11a]}$$

n=40, q^2=0.84, R^2=0.85, s=0.50, F=69

From the equation 3.11a, it can be seen that the solute's molecular volume (V_w, an expression of its hydrophobicity) and H-bond acceptor basicity (β) are the main factors governing the retention of solutes on XBridge™ Shield RP_{18} stationary phase. On the other hand, the influence of dipolarity/polarizability (**π***) is small while H-bond donor acidity (**α**) is trivial.

To compare between the log K_w values obtained with the XBridge™ Shield RP_{18} stationary phase and the log P_{oct} values of the same set of compounds, the log P_{oct} were also analyzed by LSERs as in equations 3-12 and 3-12a.

$$\textbf{log } P_{oct} = 2.76\ 10^{-2}\ (\pm0.35\ 10^{-2})\ V_w - 0.83\ (\pm0.40)\ \pi^* - 2.06(\pm0.55)\ \beta - 0.05(\pm0.55)\ \alpha - 0.26(\pm0.55) \quad \textbf{[3-12]}$$

n=40, q^2=0.90, R^2=0.91, s=0.43, F=86

After removal of the non-significant variable α,

$$\textbf{log } P_{oct} = 2.76\ 10^{-2}\ (\pm0.34\ 10^{-2})\ V_w - 0.84\ (\pm0.37)\ \pi^* - 2.05\ (\pm0.53)\ \beta - 0.25\ (\pm0.54) \quad \textbf{[3-12a]}$$

n=40, q^2=0.90, R^2=0.91, s=0.42, F=118

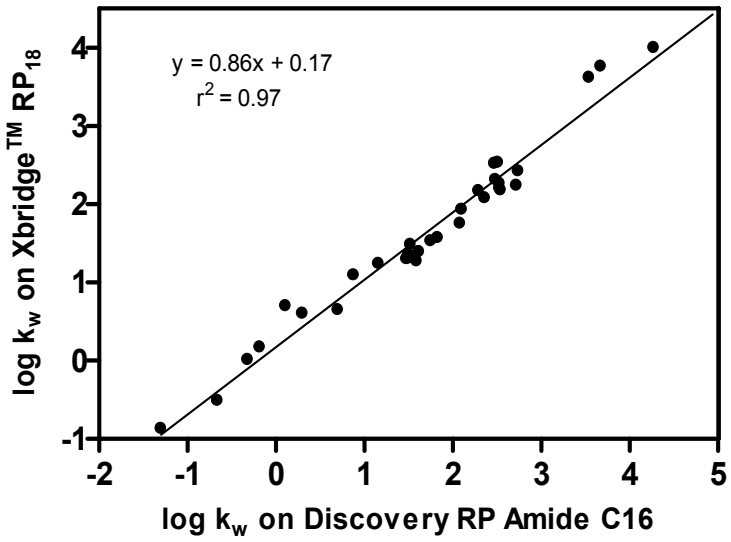

Figure 3.5. Relationship between log K_w values obtained with the XBridge^{TM} Shield RP_{18} and Discovery RP Amide 16 stationary phases (the data for discovery RP Amide 16 were cited from reference (*97*).

It is also clear from equation 3.12a that also α has no significance and π* is less significance, while V_w and β are the two main structural properties that govern the partitioning mechanism in n-octanol/water. This means that the same balance of intermolecular forces is encoded by log P_{oct} and log K_w measured on the XBridge^{TM} Shield RP_{18} phase. This finding indicates the high significant correlation between these two parameters as shown in equation 3-8.

3.3 Temoporfin (mTHPC) Transfer between Liposomal Membranes

3.3.1 Method Validity

The donor and acceptor liposomes prepared by extrusion through a 100 nm polycarbonate membrane had polydispersity indices less than 0.10 indicating a high homogeneity of the vesicle sizes. During the time of use of the formulations for the transfer experiments, there were virtually no changes in the particle sizes and polydispersity values. More than 93 % of the donor liposomes were unilamellar, the remaining small fraction showing only bilamellarity.as shown from figure 3.6. In order to evaluate the validity of the method in terms of donor retention and acceptor recovery, a control experiment was carried out using non-exchangeable markers. With pre-equilibrated columns, 99% of donor liposomes (charged vesicles) were retained as shown in figure 3.7a. For the acceptor liposomes (neutral vesicles),

91-99% were recovered in the eluate (see figure 3.7b). Acceptor recovery is a significant improvement over the recoveries (40-70%) reported by van den Besselaar et al. (*85*) and recoveries (80-95%) obtained by McLean and Phillips (*43*).

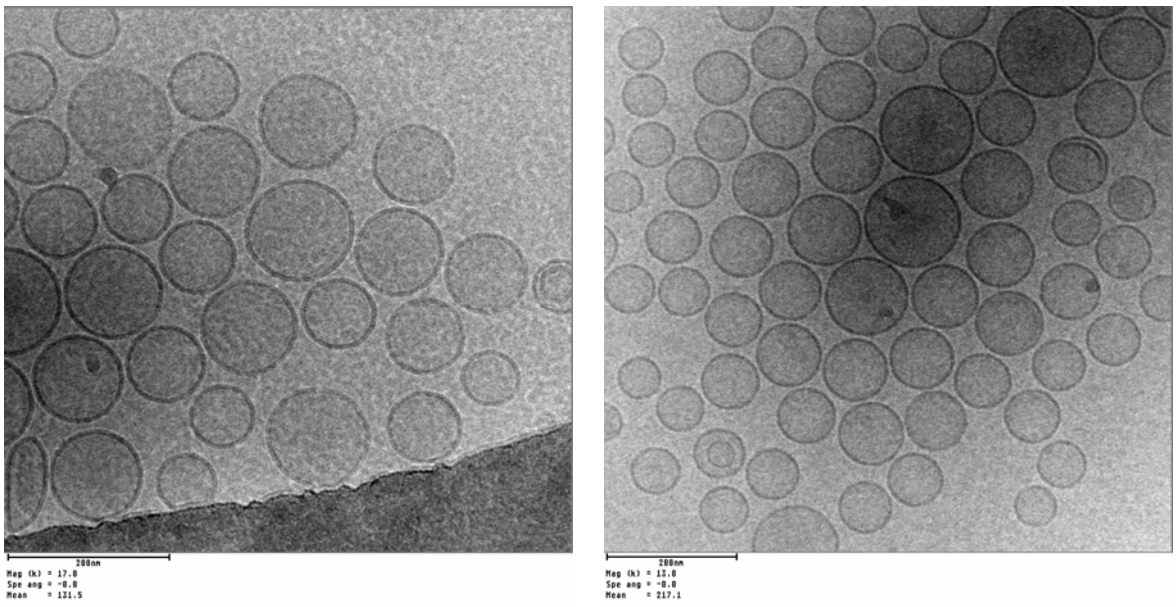

Figure 3.6. Cryo-Transmission Electron Microscopy of large unilamellar liposomes (these pictures done by Frank Steiniger, FSU Jena)

3.3.2 Effect of Total Lipid Content on [^{14}C]mTHPC Transfer Kinetics

Because the release of drug from a drug delivery system is an important step in the inter-membrane transfer of lipophilic drugs, the assessment of the release kinetics can be predictive for the adsorption parameters of the drugs (*35*). It is well known, that with increasing incubation time, photosensitizers (temoporfin) can migrate from the plasma membrane to the more sensitive stores within the cell (*70*). Temoporfin was observed to accumulate in mitochondria of myeloid leukemia cells (*98*). In this work, liposomes were used as a model of biological membranes. For better mimicking the lipid composition of biological membranes; cholesterol has been added in all cases. It must be pointed out, that 20 mol % of cholesterol has been chosen in order to avoid drastic changes of the liposome main properties: at cholesterol concentration lower than 33 mol % of the total lipid moles, no effect is observed on the size of liposomes and the phase transition is not inhibited (*99*).

To identify the mTHPC transfer mechanism, the rate of transfer was examined over a range of total lipid concentrations. Table 3.4 and figure 3.8 report the results of mTHPC transfer

experiments in which the donor: acceptor vesicle ratio was kept constant, while the total lipid concentration was varied.

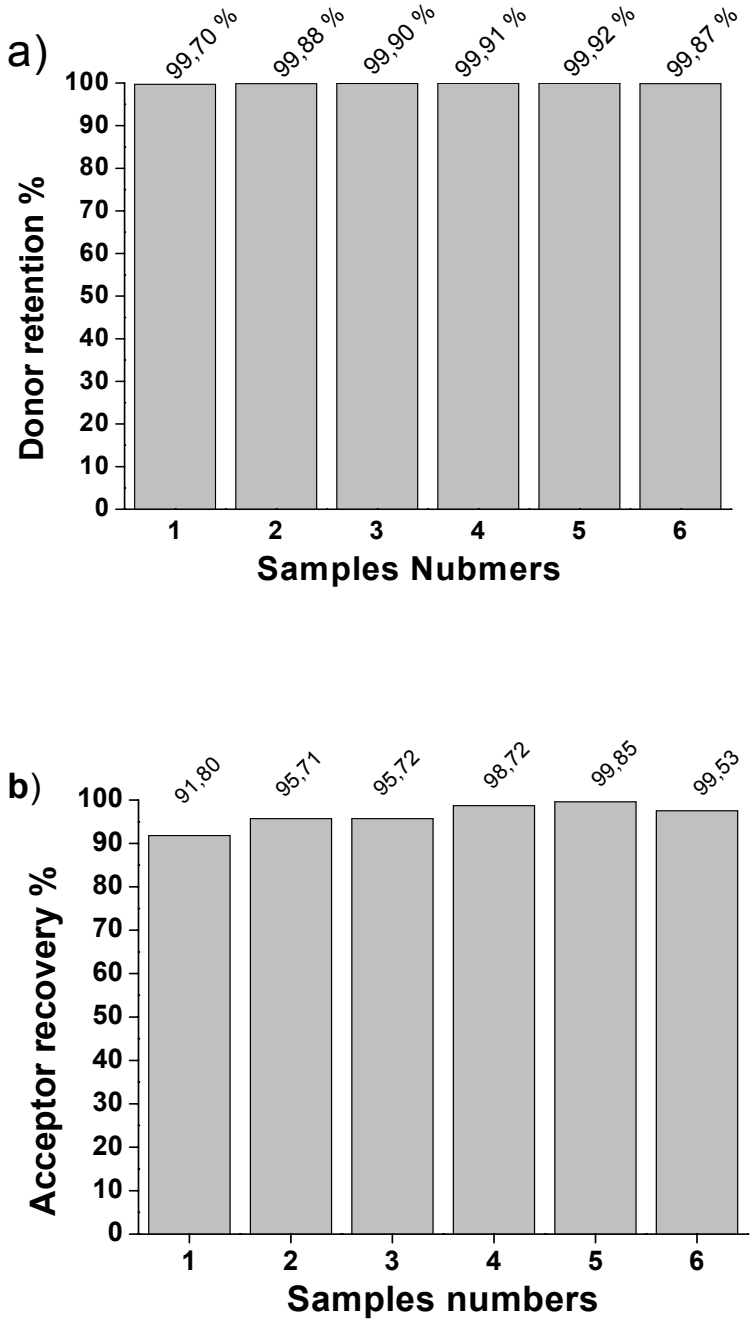

Figure 3.7. (a) Donor retention % and (b) Acceptor recovery % in ion-exchange micro-column model based drug transfer experiments using negatively charged liposomes as donor (DMPC/DCP/Chol, 7:1:2) and neutral liposomes as acceptor (POPC/Chol, 8:2).

The transfer (figure 3.8a) can be described very well by a simple exponential function. To compare with the transfer model presented in the appendix, in figure 3.8b the rate constant K as a function of the total lipid concentration have been plotted (as stated in table 3.4). Also a linear fit is shown in figure 3.8b, which relates the experimental data to the theoretically predicted relation for K. The fit exhibits both a finite slope and finite intercept, suggesting that transfer through both diffusion and collision mechanisms could contribute to the experimentally observed data. However, the reliability of this interpretation is weakened by small number of data points and by the basic model (see appendix). In particular, the possible non-ideality of the mixture of drug molecules in donor and acceptor vesicles (including self-assembly and aggregation phenomena) is not accounted for by the theoretical model in the appendix or by any other previous modelling attempt. There is clearly a need to develop and make available more elaborate modelling approaches. The model in the appendix does not account for the small offset at t = 0 as well (for example visible in figure 3.8 and figure 3.10). This may be due to drug bound to the surface, which can be transferred fast to the acceptor liposomes.

The inter-membrane transfer phenomenon was firstly described as part of membrane biochemistry studies with liposomes as model membranes for biological membranes (*35*). The assessment of inter-membrane transfer properties yields valuable information about the use of liposomes as solubilisers or as targeting devices for lipophilic drugs. In addition, the transferring properties may be predictive to some extent for the distribution and retention kinetics of drugs in the biomembranes after parenteral administration (*35*). It is well known that with increasing incubation time, photosensitizers (temoporfin) can migrate from the plasma membrane to the more sensitive stores within the cell (*70*).

Table 3.4. Total lipid, rate constants, half lifes, and maximum percentage transferred of temoporfin transfer regarding total lipid content.

Total lipid mg/ml	K hr^{-1}	$t_{1/2}$ hr	Max.% transferred
1.1	0.19 ± 0.02	3.65	74.70
11	0.28 ± 0.03	2.48	79.39
22	0.40 ± 0.04	1.73	86.34

Donor liposomes (DMPC/DCP/Chol.= 7:1:2) were 110 nm with PDI 0.06, Z-potential –33.4mV, and preloaded with ^{14}C-temoporfin. Acceptor liposomes (POPC/Chol. = 8:2) were 115 nm with PDI 0.04 and Z-potential 0.36mV. The ratio of donor lipid to acceptor lipid was 1:10 mg/mg. The molar drug: donor lipid ratio was 1:867.

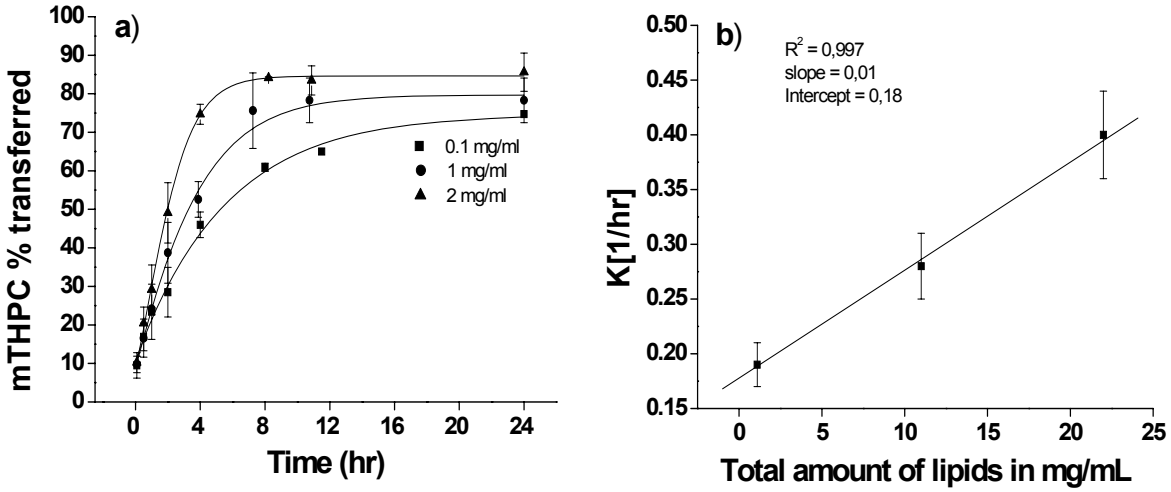

Figure 3.8. a) Temoporfin transfer between liposomes at three different lipid concentrations at 37 °C (±1). Donor liposomes (DMPC/DCP/Chol = 7:1:2) were 110 nm with PDI 0.06, Z-potential –33.4mV, and preloaded with ^{14}C-temoporfin. Acceptor liposomes (POPC/Chol = 8:2) were 115 nm with PDI 0.04 and Z-potential 0.36mV. The ratio between donor and acceptor was 1:10. Error bars represent ± SEM for six aliquots in two experiments. b) Calculated total lipid content plotted versus transfer constants (see table 3.4).

Previously, two different models have been suggested to explain the transfer of lipophilic or amphiphilic membrane components between two lipid domains (either inter-membrane transfer or transfer from membrane to, e.g. plasma components). The first model proposes a collision mechanism for, e.g. phosphatidylcholine (*100*) and cholesterol transfer (*101*). The second model postulates transfer through the water phase as demonstrated by cholesterol transfer (*43, 102*) and phosphatidylcholine transfer studies (*43*). Others claim that both mechanisms may simultaneously play a role, as demonstrated by the transfer of monoacylglycerols from SUV's to brush border membrane vesicles (*103*). The kinetic equations describing both transfer mechanisms (through liposome collisions and through diffusion via the water phase) are derived in the Appendix. This derivation is based on a detailed distribution function of drug molecules among donor and acceptor vesicles. A similar derivation, although without considering the distribution of drug molecules among donor and acceptor liposomes, was suggested previously by Jones and Thompson (*100*). In both models, lipid transfer between liposomes through the aqueous phase via desorption from the bilayer is

described by a “First Order Model”. In contrast, the transfer upon the collision of liposomes (donor-donor, donor-acceptor, or acceptor-acceptor) corresponds to a “Second Order Model”. As we show in our appendix, both lead to an exponential transfer kinetics with an apparent rate constant K = Kd + cKc where Kd and Kc are constants and c is the total liposome concentration. (As we show in the appendix, there is an additional dependence of K on the ratio between the total number of drug molecules in the system and the maximal number of drug molecules that all liposomes are able to carry. This dependence is only relevant to liposomes with maximal, or near maximal, drug loading. For figure 3.8 the molar drug:donor lipid ratio was 1:867, sufficiently far away from the maximal ratio 1:10 (*104*). It is emphasized that only the collision mechanism leads to a dependence on the total liposome concentration c. Figure 3.8b shows the dependence of the apparent rate constant K on the total lipid concentration. The finite slope and finite intercept of the linear fit suggest that both the diffusion and collision mechanisms are involved in the transfer process.

Comparison on the linear fit in figure 3.8b with the relation K = Kd + c Kd yields Kd = 0.18/hr and Kc = 0.01 m_L ml/(mg hr) where m_L is the mass of a single liposome. The vesicles in this experiments have a radius of roughly R= 50 nm. Assuming a cross-sectional area a = 0.7 nm^2 per lipid, this implies a number of $\frac{2.4.\pi.R^2}{a}$ = 90000 lipids per liposome (where the additional factor of 2 accounts for the two leaflets of the liposomal membrane). The molar mass per lipid is roughly 700 g/mol. Hence, m_L= 700 g/mol 90000 = 10^{-13} mg. Kc estimation then becomes Kc = 0.01 m_L ml/(mg hr) =10^{-3} μm^3/hr. The liposome concentration c in K = Kd + cKd can be stated conveniently in ``number of liposomes/μm^3''. Here, estimation for Kd and Kc imply that up to a liposome concentration of c = Kd/Kc = 180/μm^3 the transfer is dominated by the collision mechanism. In other words, once the average center-to-center distance between neighbouring liposomes is larger than about 200 nm, diffusion through the aqueous phase becomes the predominant transfer mechanism. It should be noted that the final estimation Kd = 0.18/hr and Kc = 10^{-3} μm^3/hr are subject to the assumptions of underlying theoretical model in the appendix, namely that the mixture of mTHPC in each individual liposome is ideal. This neglects other possible rate limiting physical mechanisms such as aggregation and self-assembly of mTHPC inside the liposomes. Hence, this study suggests the transfer of mTHPC via both a diffusion and collision mechanism, subject to the (yet not verified) assumption that interactions of the drug molecules inside the liposomes do not limit the rate of transfer.

3.3.3 Effect of Temperature on [^{14}C]mTHPC Transfer Kinetics

The obtained results of the experiments designed to examine the sensitivity of transfer rate constants to temperature are presented in table 3.5 and figure 3.9. The sensitivity of the transfer rate on the phase transition temperature (22 °C) for DMPC can be easily seen. In the chosen temperature range (15-37 °C), an increase in the transfer rate constants and the maximum amount transferred was detected. The apparent transfer rates were 0.05 ± 0.01 hr^{-1}, 0.07 ± 0.01 hr^{-1}, 0.09 ± 0.01 hr^{-1}, 0.12 ± 0.04 hr^{-1}, 0.17 ± 0.04 hr^{-1}, and 0.24 ± 0.04 hr^{-1} while the plateaus reached at 24.35, 34.32, 51.50, 60.20, 70.44, and 88.41 % at 15, 19, 22, 25, 30, and 37 °C respectively. From the observed transfer rates it is evident that the transfer rate has almost doubled by increasing the temperature by 10 °C. From the van't Hoff plot of apparent transfer coefficient ln $K_{D\rightarrow A}$ versus T^{-1} over the temperature range 15-37 °C, the enthalpy ΔH was (+96.18 KJ mol^{-1}), the entropy ΔS (+324.17 J mol^{-1} K^{-1}) and the free energy ΔG (– 4.31.KJ mol^{-1}) could be estimated. A plot of log K over 1/T (see figure 3.9b) suggests two different linear regimes, separated by the main phase transition temperature (22 °C) of DMPC which is the major lipid in the donor liposomes. The corresponding fits to the Arrhenius equation yield activation energies of 56 kJ/mol below the main transition temperature and 44 kJ/mol above the main transition temperature. The somewhat smaller activation energy in the fluid phase state may reflect a less severe perturbation of the lipid matrix upon transferring mTHPC from the hydrocarbon core of the lipid bilayer into the aqueous region outside the membrane. It well documented that molecular motion in general and acyl chain mobility in particular increases with temperature resulting in a more fluid membrane environment. Although a drug apparently favours a more fluid bilayer arrangement, the rate of transfer and the maximum amount transferred increased when the lipid membranes were heated (see table 3.5 and figure 3.9). Moreover, the transfer rate constant of mTHPC at 37 °C is about 5-fold higher than at 15 °C which might lead to the rapid release of mTHPC at body temperature. This may be ascribed to the decrease of the hydrophobic interaction strength between the lipid and the drug when the temperature is increased, thus resulting in higher aqueous solubility of mTHPC. In agreement with the study of Wenk et al. (*105*) regarding paclitaxel (Taxol®) partitioning into lipid bilayers, the binding of paclitaxel to liposomes is four times stronger at 20 °C than at 37 °C. In contrast, the aqueous solubility of cyclosporine A increases with decreasing the temperature. This might cause problems in stability-related issues of cyclosporine A liposomal formulations, as cyclosporine A can partition out of the liposomal membrane and form crystals in the suspending medium (Fahr, unpublished results). Another explanation for the temperature-related effects may be provided by the thermally-induced

changes in the conformation of the head group. It has been suggested that the N^+ end of the phosphocholine dipole of PC, which lies parallel to the bilayer surface, becomes increasingly

Table 3.5. Rate constants, have lives and maximum percent transferred of temoporfin transfer regarding temperature and donor vesicle's charge.

Temperature							**Donor Vesicle's Charge**	
Temp. (°C)	15°C	19°C	22°C	25°C	30°C	37°C	– Ve D.	+ Ve D.
K hr^{-1}	0.05 ± 0.01	0.07 ± 0.01	0.09 ± 0.01	0.12 ± 0.04	0.17 ± 0.04	0.24 ± 0.04	0.26 ± 0.03	0.43 ± 0.06
$t_{1/2}$ hr	13.86	9.9	7.70	5.80	4.08	2.89	2.67	1.61
Max. % transferred	24.35	34.32	51.50	60.20	70.44	88.41	65.31	72.29

Donor liposomes (DMPC/DCP/Chol = 7:1:2) were 90 nm (PDI 0.08), Zeta-potential –33.4mV, and preloaded with temoporfin. Acceptor liposomes (POPC/Chol. = 8:2) were 115 nm (PDI 0.04) and Zeta-potential 0.36mV. For the comparison between oppositely charged donor liposomes (at 37°C), the negatively charged ones were comprised of DOPC/DCP/Chol; 7:1:2, while positively charged ones were prepared from DOPC/DOTAP/Chol 5:3:2. Acceptor liposomes (POPC/Chol. = 8:2) were 115 nm with (PDI 0.04) and Zeta-potential -0.36mV. Donor lipid concentration was 1mg/mL while acceptor lipid concentration was 10mg/mL. The molar drug:donor lipid ratio was 1:867. The ratio between donor and acceptor was 1:50 in order to achieve sink conditions.

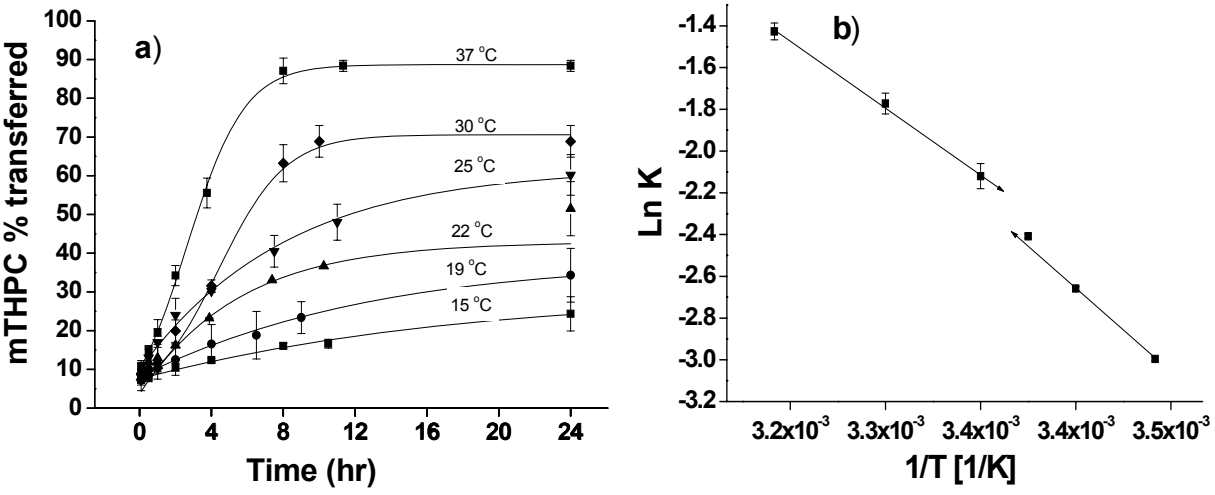

Figure 3.9. a) Temoporfin transfer between liposomes at four representative temperatures 15, 19, 22, 25, 30, and 37 °C (±1) from 3.6. Donor liposomes (DMPC/DCP/Chol = 7:1:2) were 90 nm (PDI 0.08), Zeta-potential -33.4 mV, and preloaded with temoporfin. Acceptor liposomes (POPC/Chol = 8:2) were 115 nm (PDI 0.04) and Zeta-potential -0.36mV. Error bars represent ± SEM (n=9). The molar drug:donor lipid ratio was 1:867. b) Arrhenius plot of all temperature points from table 3.6 and stepwise fit to the Arrhenius equation.

submerged in the hydrocarbon chain with increasing temperature, which results in lateral head group repulsion and decreasing surface pressure. The reduction of surface pressure may be expected to favour transfer (*106*). Another possible explanation for these temperature related effects may be found by thermodynamic considerations. When the temperature increases the enthalpy of transfer becomes more positive and the free energy of transfer less favourable which in turn enhances the water solubility of hydrophobic solutes like mTHPC. Counterbalancing this effect the incorporation of non-polar molecules like mTHPC across and into interfacial membrane bilayer is thought to be the result of the hydrophobic effect, which, in turn, is driven by entropic factors (*107*). The positive entropy of solutions which promotes drug transfer from aqueous phase into hydrophobic domains, is believed to result from the dissolution of an ordered water shell around the drug (*108*). In the present study, the positive value of the enthalpy ($\Delta H = +96.18$ kJ mol^{-1}) may increase the release of mTHPC from donor lipid phase to the aqueous phase. After that, the positive entropy ($\Delta S = +324.17$ J mol^{-1} K^{-1}) of the solution promotes mTHPC to be transferred into the acceptor since the acceptor lipid to donor lipid is 10:1 mg/mg. It could be concluded from the positive values of entropy a ΔS and the negative value of the free energy ΔG that mTHPC transfer over the temperature range of 15-37 °C is entropically dominated. It is interesting also to discuss the prediction of a kinetic model, presented in the appendix, for the free energy of transfer ΔG (see equation 2-10). To this end, it should be noted from the model in the appendix that the model assumes all liposomes to be equivalent (i.e. mTHPC is assumed to have the same standard chemical potential in donor and acceptor vesicles). The enthalpic contribution ΔH to ΔG therefore vanishes. On the other hand, the equilibrium constant $K_{D->A} = Na/Nd$ is given in our model by the ratio of the numbers of acceptor to donor liposomes. Then, with equations 4 and 5 and using the experimentally fixed ratio Na/Nd = 10 (see table 3.5), we find $\Delta G = -RT \ln (Na/Nd) = -5.7$ kJ/mol, which is in reasonable agreement with the experimentally determined value $\Delta G = -4.31$ kJ/mol. Although these experiments reveal the presence of an enthalpic contribution to ΔG, the transfer is dominated by entropy. This provides a major justification for the assumption of constant standard chemical potential in the kinetic model.

3.3.4 Effect of Donor Liposome's Charge on [^{14}C]mTHPC Transfer Kinetics

To investigate the role of donor liposome charge on the mTHPC transfer rate, we used binary lipid mixtures as compiled in table 3.5. These mixtures are composed of DOPC either with DOTAP or with DCP to prepare positively and negatively charged vesicles, respectively. From table 3.5 and figure 3.10 we conclude, that positively charged liposomes exhibit faster

transfer rates than negatively charged liposomes. The observed transfer rate of positively charged vesicles (0.43 ± 0.06 hr^{-1}) was about 1.7-fold of the negatively charged ones (0.26 ± 0.03 hr^{-1}). A possible reason for this finding may be related to the influence of charged lipids on physical membrane properties. Binary anionic/zwitterionic and cationic/zwitterionic lipid mixtures exhibit characteristic differences in terms of their average cross-sectional area per lipid, head group orientation, and interaction strengths as evidenced by experiments (*109-111*), Molecular Dynamics simulations (*112*), and mean-field electrostatic modelling (*113, 114*). Generally, cationic lipids tend to electrostatically interact more strongly with zwitterionic lipids due to the typically close proximity of the cationic charge to the phosphate group of the zwitterionic lipid. Hence, mixed cationic/zwitterionic membranes are more condensed than their anionic counterparts, which suggest a less favourable packing environment of drug molecules inside the membrane and a larger driving force for the transfer out of the membrane interior. In terms of the maximum amount transferred, there is no significant difference between the both as 65.31 % and 72.29 % for negatively and positively charged liposomes were transferred, respectively.

3.3.5 Effect of Donor Lipid Saturation and Acyl Chain Length on [^{14}C]mTHPC Transfer Kinetics

The effect of degree of saturation of lipid used in donor vesicles is presented in table 3.6 and figure 3.11. It is evident that there is no significant difference between transfer rate constants 0.26 and 0.18 hr^{-1} of DOPC (18:1/18:1, T_m = –20) and SOPC (18:0/18:1, T_m = +6) respectively. While for DSPC (18:0/18:0, T_m = +55) was about 4-fold of each (1.00 hr^{-1}). Since membrane rigidity is increased with increasing the degree of hydrocarbon saturation, a potential relationship between transfer rate and rigidity was evident. The maximum amount transfer percents were 65.31, 83.63, and 82.01 for DOPC, SOPC, and DSPC respectively. As an extension of the former experiment, the influence of fatty acyl chain length was examined. With the four di-saturated phospholipids used [(DMPC 14:0/14:0, Tm = +22 °C), (DPPC 16:0/16:0, Tm = +41 °C), (DSPC 18:0/18:0, Tm = +55 °C), and (DBHPC 22:0/22:0, Tm = +75 °) the transfer rate was faster for the phospholipid having longer length at 37 °C which was either below or above their respective phase transition temperatures (table 3.6 and figure 3.12). It is obvious that there is no significant difference between the transfer rate of DMPC (0.28 ± 0.03 hr-1) and DPPC (0.35 ± 0.03 hr-1). The transfer rate constants for DSPC and DBHPC increased to about 4-fold (1.00 ± 0.11 hr-1 and 1.24 ± 0.30 hr-1 respectively). The

maximum amount transferred was almost the same as the plateaus were reached at 79 %, 86 %, 82 %, and 75 % for DMPC, DPPC, DSPC, and DBHPC respectively.

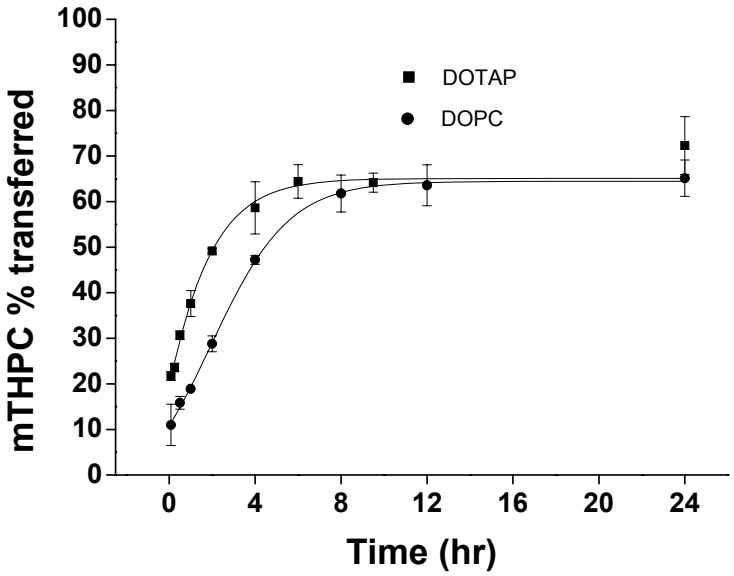

Figure 3.10. Temoporfin transfer between negatively and positively charged donor and neutral acceptor liposomes at 37 °C (± 1 °C). Donor liposomes formulated as (DOPC/DCP/Chol.= 7:1:2) and (DOPC/DOTAP/Chol = 5:3:2 loaded with temoporfin. Acceptor liposomes (POPC/Chol = 8:2) were 115 nm (PDI 0.04) and Zeta-potential -0.36mV. The ratio between donor and acceptor was 1:10. Error bars represent ± SEM (n = 6). The molar drug:donor lipid ratio was 1:867.

The overall affinity of the porphyrin for the vesicles is largely dominated by hydrophobic interactions between the macrocycle core and the phospholipid chains. Two of the chain's characteristic factors are the unsaturation and acyl chain length. A sharp increment in mTHPC transfer rates was shown only by using DSPC (Tm = +55 °C) and DBHPC (Tm = +75 °C). Below the phase transition temperature a potential relationship between transfer rate and rigidity is evident. As presented in table 3.6 and figures 3.12b, there is no significant difference between transfer rate constants for DOPC (Tm = -20 °C), SOPC (Tm = +6 °C), DMPC (Tm = +22 °C), and DPPC (Tm = +41 °C), whereas for DSPC (Tm = +55 °C) and DBHPC (Tm = +75 °C), the transfer rate was increased by about a factor of 4. The experiments were conducted at a temperature of 37 °C at which DOPC, SOPC, and DMPC

reside in the fluid phase state whereas DPPC tends to form the “ripple” phase. In contrast, membranes containing DSPC and DBHPC exhibit the gel phase, where the fully stretched and well packed fatty acyl chains give rise to more rigid membrane architecture. This could cause the drug molecules to be squeezed out of the bilayer interior and to accumulate near the liposome surface (*35*). This would increase the probability of being transferred to another membrane, as desorption of the drug from the liposomes becomes easier. A rapid release of a hydrophobic drug (Vitamin A) was also observed for solid lipid nanoparticles (*115*), the classic example of a rigid lipidic matrix. It was shown for these rigid carriers (*116*), see also the review in reference (*117*), that the mere lipophilicity of carrier and drug does not necessarily cause a retardation effect. Only if there is a structural fit between carrier assembly and drug is a retardation effect to be expected (*117*). For less rigid carriers such as liposomes in their fluid state, the structural fit may be provided by the ability of the fluid-like lipid tails to adapt to the shape of the hydrophobic drug molecule. Such accommodation would be expected to be weakly dependent on chain length, as is observed. However, this effect is overridden by the rigidity of the membrane, as exemplified by the case of DBHPC. Maman and Brault (*118*) report, that varying the bilayer thickness by using C14-C22 unsaturated phospholipids at pH 6.5, a profound decrement in dicarboxylic porphyrin transfer rate was observed. They ascribed this influence to the length of the hydrocarbon chain since all of unsaturated lipids used in their report are liquid at their experimental temperature 25 °C, thereby the degree of burying porphyrin within the bilayer will be high. In a study of anticancer teniposide partitioning into membranes using different lipids regarding unsaturation and acyl chain length at 37 °C, Stephan and co-workers found that the partitioning coefficient was decreased when the membrane rigidity increased having the lowest partitioning coefficient recorded for DSPC (*108*), which is also supporting this notion.

Table 3.6. Phase transition temperatures, Z-averages, rate constants, half lifes and maximum percent transferred of temoporfin transfer regarding donor lipid saturation and donor lipid acyl chain length at 37 ^{o}C.

	Unsaturation			Acyl chain length			
Lipid	DOPC	SOPC	DSPC	DMPC	DPPC	DSPC	DBHPC
T_m (^{o}C)	-20	+6	+55	+22	+41	+55	+75
Z-average	88.0	89.0	100.9	110	100.8	100.9	168.3
K hr^{-1}	0.26 ± 0.03	0.18 ± 0.01	1.00 ± 0.11	0.28 ± 0.03	0.35 ± 0.03	1.00 ± 0.11	1.24 ±0.30
$t_{1/2}$ hr	2.67	3.85	0.69	2.48	1.98	0.69	0.56
Max. % transferred	65.31	83.63	82.01	79.39	86.38	82.01	75.51

Donor liposomes (PhL/DCP/Chol.= 7:1:2) preloaded with temoporfin had PDIs less than 0.10. Acceptor liposomes (POPC/Chol. = 8:2) were 115 nm (PDI 0.04) and Zeta-potential -0.36mV. The donor lipid concentration was 1mg/mL while for acceptor was 10mg/mL The molar drug:donor lipid ratio was 1:867.

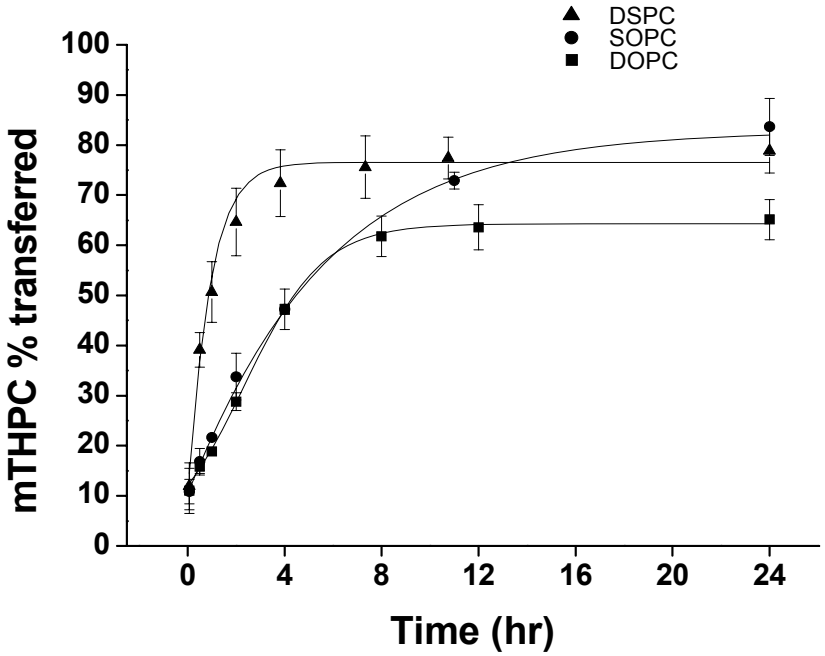

Figure 3.11. Temoporfin transfer between liposomal membranes regarding hydrocarbon chain saturation (DOPC, SOPC, and DSPC) at 37 ^{o}C (±1). Donor liposomes formulated as (PhL/DCP/Chol = 7:1:2) and loaded with ^{14}C-temoporfin. Acceptor liposomes (POPC/Chol = 8:2) were 115 nm with PDI 0.04 and Z-potential 0.36mV. The ratio between donor and acceptor was 1:10. Error bars represent ± SEM for six aliquots in two experiments for DOPC and SOPC while for DSPC for nine aliquots in three experiments.

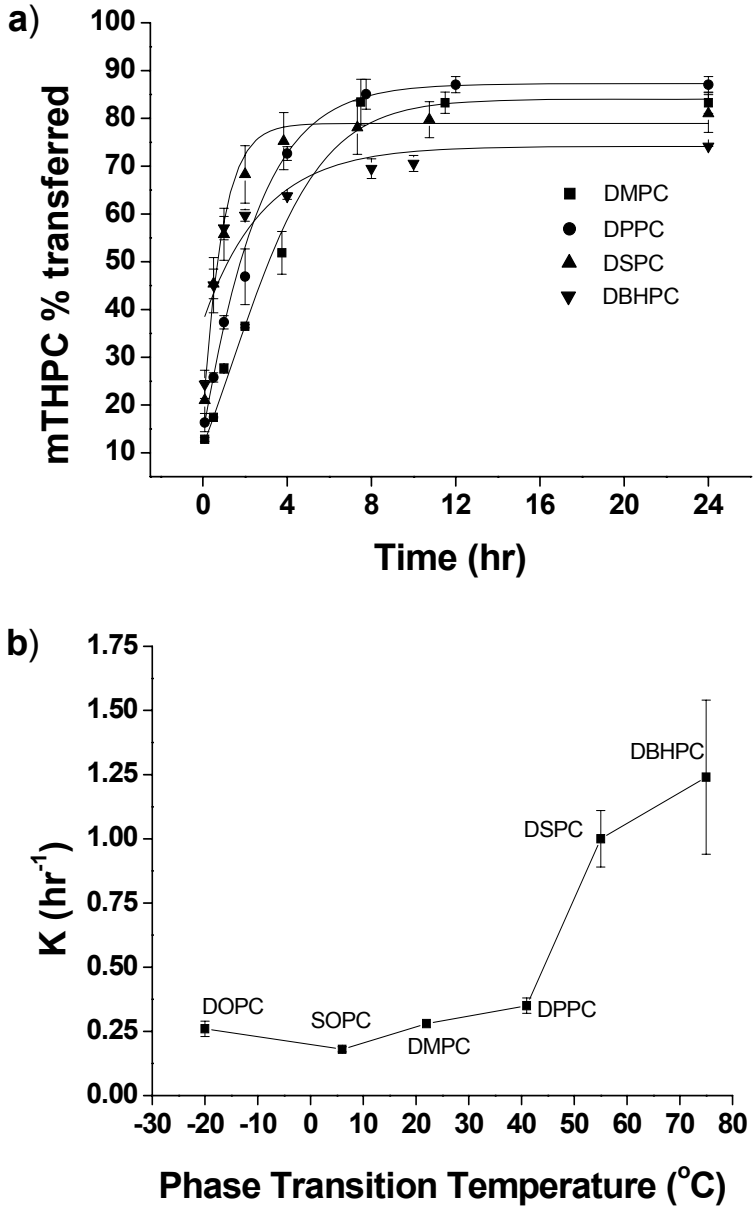

Figure 3.12. a) Temoporfin transfer between liposomal membranes regarding carbon chain length (DMPC, DPPC, DSPC, and DBHPC) at 37 ^{o}C (±1). Donor liposomes formulated as (PhL/DCP/Chol = 7:1:2) and loaded with ^{14}C-temoporfin. Acceptor liposomes (POPC/Chol = 8:2) were 114.8nm with PDI 0.04 and Z-potential 0.36mV. The ratio between donor and acceptor was 1:10. Error bars represent ± SEM for six aliquots in two experiments for DMPC and DPPC while for DSPC and DBHPC nine aliquots in three experiments. b) Rate constants as a function of the phase transition temperature of the donor liposome of six different phospholipids regarding saturation and fatty acyl chain length (Data taken from table 3.7).

PART IV
CONCLUSIONS

4. CONCLUSIONS

4.1 Immobilized Artificial Membrane (IAM.PC.DD2)

The retention behaviour of a set of neutral and positively or negatively charged solutes on the IAM.PC.DD2 stationary phase was compared to traditional lipophilicity index log P_{oct}. Significant correlations were found between the retention factor log k_{wIAM} on this stationary phase and log P_{oct} or log $D_{7.0}$ for neutral or structurally related compounds, implying that the retention mechanisms are the same for neutral or structurally related compounds. The retention of the ionized compounds on the IAM.PC.DD2 is controlled not only by lipophilicity but also by extra interactions, mainly electrostatic interactions between charged solutes and phospholipids. For the solutes investigated in this study, positively charged compounds are more retained than negatively charged solutes. The ranking order of retention strength is: β-blockers > (4-methylbenzyl) alkylamines > NSAIDs > monofunctional carboxylic acids. This implies that the interaction between positively charged solutes and the phosphatidylcholine-based IAM stationary phase is larger than that between negatively charged solutes and the membrane, and that the electrostatic interaction depends on the structural characteristics of the solutes investigated.

4.2 XBridge^{TM} Shield RP_{18} Stationary Phase

Using a wide range of structurally diverse neutral, acidic, ampholytic and basic solutes (including drugs) and eluents enriched in 1-octanol, the Xbridge^{TM} shield RP_{18} phase yielded a lipophilicity index log K_w highly correlated with log P_{oct} values. An LSERs analysis showed that retention on the Xbridge^{TM} shield RP_{18} phase and partitioning in 1-octanol/ water are controlled by the same balance of structural properties, namely Van der Waals volume (V_w), H-bond acceptor basicity (β) and dipolarity/polarizability (π^*). The study showed that this novel stationary phase overcomes the shortcomings of the silica-based stationary phases, whose application in lipophilicity measurements is limited to neutral and acidic compounds. The results of this study are of potential interest for the high-throughput screening of lipophilicity in drug discovery, where basic compounds predominate.

4.3 Temoporfin (mTHPC) Transfer between Liposomal Membranes

The kinetics of transfer of the hydrophobic drug temoporfin from donor to acceptor liposomes was discussed. The results showed that the transfer rates depend not only on thermodynamic parameters such as temperature and concentrations of donor and acceptor vesicles, but also characterize it in terms of liposomal material properties. The observed transfer kinetics

generally follows a simple exponential behaviour with a corresponding rate constant that contains information about the mechanism of transfer. A theoretical model that analyzes the transfer based on a detailed distribution function of drug molecules in liposomes was presented. The model accounts for drug transfer through liposome collisions and via diffusion through the aqueous phase. Comparison of the theoretically predicted with the measured rate constants suggests that both mechanisms contribute to the transfer. The collision mechanism dominates for large overall liposome concentration (larger than about $1/(200\ \text{nm})^3$). The model gives also reasonable agreement for the (entropy-dominated) free energy of transfer of temoporfin from the donor to the acceptor liposomes.

PART V
Appendix

5. Appendix

This appendix describes a kinetic model that predicts an exponential transfer curve and includes both a diffusion-based and a collision-based transfer mechanism. The model is microscopic in the sense that it explicitly accounts for the distribution of [^{14}C]mTHPC in donor and acceptor liposomes. Specifically, we introduce the numbers $d=d_j(t)$ and $a_j=a_j(t)$ of, respectively, donor and acceptor liposomes that contain j molecules of [^{14}C]mTHPC. The index j varies in the region $0 \le j \le$ where m is the maximal number of mTHPC that can be incorporated into a single liposome. The total number of donor liposomes $N_d = \sum_{j=0}^{m} d_j$ and the total number of acceptor liposomes $N_a = \sum_{j=0}^{m} a_j$ are both conserved. All $N=N_d+N_a$ liposomes are enclosed in a volume V at fixed temperature T. The total numbers $M_d = \sum_{j=0}^{m} jd_j$ and $M_a = \sum_{j=0}^{m} ja_j$ of mTHPC residing in, respectively, donor and acceptor vesicles are not conserved, but the sum $M=M_d+M_a$ is. A simple kinetic model of [^{14}C]mTHPC transfer among all different donor and acceptor vesicles can be written as

$$\begin{aligned}
\frac{d}{dt}dj &= \frac{K_c}{V}\left\{\sum_{i=0}^{j}(d_i+a_i)\left[d_{j+1}(j+1-i)-d_j(j-i)\right]+\sum_{i=j}^{m}(d_i+a_i)\left[d_{j-1}(i-j+1)-d_j(i-j)\right]\right\} \\
&+K_d\left[(j+1)d_{j+1}-jd_j+\frac{m-(j-1)}{m-(N/M)-1}d_{j-1}-\frac{m-j}{m(N/M)-1}d_j\right] \\
\frac{d}{dt}aj &= \frac{K_c}{V}\left\{\sum_{i=0}^{j}(a_i+d_i)\left[a_{j+1}(j+1-i)-a_j(j-i)\right]+\sum_{i=j}^{m}(a_i+d_i)\left[a_{j-1}(i-j+1)-a_j(i-j)\right]\right\} \\
&+K_d\left[(j+1)a_{j+1}-ja_j+\frac{m-(j-1)}{m(N/M)-1}a_{j-1}-\frac{m-j}{m(N/M)-1}aj\right].
\end{aligned} \qquad \textbf{[5-1]}$$

This model accounts for two different transfer mechanisms, transfer upon collisions between vesicles and transfer through diffusion via the aqueous phase. The collision and diffusion mechanisms are accounted for by the first and second lines, respectively, in the expressions for the time derivatives of d_j and a_j. Specifically, the first line accounts for all possible collisions that increase (terms with positive sign) or decrease (terms with positive sign) the number d_j (and analogous for a_j). Each term is proportional to the concentration difference of [^{14}C]mTHPC between the colliding vesicles. The rate constant K for transfer through collisions is assumed to be constant, irrespective of the nature of the collision (donor-donor, acceptor-acceptor, or donor-acceptor). The second line describes a diffusive transport through

the aqueous phase; K_d is the rate constant for the transfer of a single [^{14}C]mTHPC from a vesicle into the aqueous phase or vice versa. Note that the set of equations (1) treat all liposomes to be structurally and chemically equivalent; i.e. with donor and acceptor liposomes to have the same equilibrium concentration of [^{14}C]mTHPC. Moreover, equations (1) assume that due to its low solubility [^{14}C]mTHPC is present in the aqueous phase with negligible concentration.

Equations (1) can be expressed as kinetic equations in terms of M_d=M_d (t) and M_a=M_a(t) only. Using the above definitions for M_d and M_a we find

$$\frac{dM_d}{dt} = K\left(N_d M_a - N_a M_d\right),$$

$$\frac{dM_a}{dt} = K\left(N_a M_d - N_d M_a\right) \qquad \textbf{[5-2]}$$

with the rate constant

$$\boldsymbol{K} = \frac{K_d}{1-\frac{M}{mN}} + K_c \frac{N}{V} \qquad \textbf{[5-3]}$$

The set of equations (1) effectively describes the reversible chemical reaction $D \rightleftharpoons A$ of [^{14}C]mTHPC bound to donor (D) and acceptor (A) liposomes, with identical on and off rate constants KN_d/N *and* KN_a/N, respectively. The kinetics of this net reaction strictly follows first-order kinetics, despite the fact that the transfer via liposome collisions is based on a bimolecular reaction, namely the collision between two liposomes. However, the number of liposomes does not change with time, leaving the rate of collisions between liposomes constant. This absence of a depletion of the reactants renders the transfer first order. The present model predicts an equilibrium constant, defined in equation 2, of $K_{D\rightarrow A} = N_a/N_d$. With the initial conditions $M_d(t = 0)$=M and $M_a(t = 0)$= 0 the predicted time dependence is given by a simple exponential function

$$\frac{M_a(t)}{M} = 1 - \frac{M_d(t)}{M} = \frac{N_a}{N}\left(1 - e^{-kt}\right) \qquad \textbf{[5-4]}$$

where N_a/N is the fraction of acceptor liposomes in the system. Equations (3) and (4) represent an exact solution of the model introduces through equations (1). Clearly, there are two different regimes, corresponding to diffusion-dominated ($(N - M/m)/V << K_c/K_d$) and

collision-dominated ($(N - M/m)/V >> K_c/K_d$) transport. The observed time dependence for the [^{14}C]mTHPC transfer from donors to acceptors does not depend on the overall concentration of liposomes in the diffusion-dominated regime. In the collision-dominated regime the transfer becomes faster with increasing liposome concentration. On the other hand, a dependence of K on total number of drug molecules, M, is only encountered in the diffusion-dominated regime. Here, K increases with M. If all donor liposomes initially contain their maximal amount of drug molecules then $M = mN_d$. Here again is pointing at the simplistic level of the present model. First, it does not account for the chemical specificity of the donor and acceptor liposomes. That is, the chemical potential of drug molecules is the same in donors and acceptors. Consequently, in equilibrium all individual liposomes (donor and acceptor liposomes) carry the same number of drug molecules (as expressed by $K_{D\rightarrow A}=N_a/N_d$), and there is no enthalpic contribution to the free energy of transfer ΔG; see equation [2-10]. Second, our model does not account for nonideal mixing of drug molecules in liposomes, including possible aggregation phenomena or self-assembly. Including the difference in affinity for drug molecules of donors and acceptors as well as aggregation of drug molecules within liposomes will be the subject of future theoretical work. This model was established with the help of Prof. Dr. Sylvio May (Department of Physics, North Dakota State University, Fargo ND 58108, North Dakota, U.S.A.).

PART VI
REFERENCES

References

1. Joachim, K., Seydel, Wiese, M. (2002) Function, composition, and organization of membranes, In *Drug-Membrane Interactions* (Mannhold, R., Kubinyi, H., Folkers, G., Ed.), pp 1-34, Wiley-VCH verlag GmbH, Weinheim.

2. Joachim, K., Seydel, Wiese, M. (2002) Drug-Membrane Interaction and Pharmacokinetics of the Drugs, In *Drug-Membrane Interactions* (Mannhold, R., Kubinyi, H., Folkers, G., Ed.), pp 141-215, Wiley-VCH verlag GmbH, Weinheim.

3. He, Y. L., Murby, S., Warhurst, G., Gifford, L., Walker, D., Ayrton, J., Eastmond, R., and Rowland, M. (1998) Species differences in size discrimination in the paracellular pathway reflected by oral bioavailability of poly(ethylene glycol) and D-peptides, *J Pharm Sci-Us 87*, 626-633.

4. Madara, J. L., and Dharmsathaphorn, K. (1985) Occluding Junction Structure-Function Relationships in a Cultured Epithelial Monolayer, *J Cell Biol 101*, 2124-2133.

5. Lampidis, T. J., Kolonias, D., Podona, T., Israel, M., Safa, A. R., Lothstein, L., Savaraj, N., Tapiero, H., and Priebe, W. (1997) Circumvention of P-GP MDR as a function of anthracycline lipophilicity and charge, *Biochemistry-Us 36*, 2679-2685.

6. Smith, Q. R., Momma, S., Aoyagi, M., and Rapoport, S. I. (1987) Kinetics of Neutral Amino-Acid-Transport across the Blood-Brain-Barrier, *J Neurochem 49*, 1651-1658.

7. Schanker, L. S., Tocco, D. J., Brodie, B. B., and Hogben, C. A. M. (1958) Absorption of Drugs from the Rat Small Intestine, *J Pharmacol Exp Ther 123*, 81-88.

8. Housten, J. B. U., D. G.; Bridges, J. W. A. . (1974) Reevaluation of the importance of partition Coefficients in the Gastrointestinal Absorption of Nutrients, *J. Pharmacol. Exp. Ther 189*, 244-254.

9. Dressman, J. B., Amidon, G. L., and Fleisher, D. (1985) Absorption Potential - Estimating the Fraction Absorbed for Orally-Administered Compounds, *J Pharm Sci-Us 74*, 588-589.

10. Banks, W. A., and Kastin, A. J. (1985) Peptides and the Blood-Brain-Barrier - Lipophilicity as a Predictor of Permeability, *Brain Res Bull 15*, 287-292.

11. Levin, V. A. (1980) Relationship of Octanol-Water Partition-Coefficient and Molecular-Weight to Rat-Brain Capillary-Permeability, *J Med Chem 23*, 682-684.

12. Rim, S., Audus, K. L., and Borchardt, R. T. (1986) Relationship of Octanol Buffer and Octanol Water Partition-Coefficients to Trans-Cellular Diffusion across Brain Microvessel Endothelial-Cell Monolayers, *Int J Pharmaceut 32*, 79-84.

13. Taillardat-Bertschinger, A., Carrupt, P. A., Barbato, F., and Testa, B. (2003) Immobilized artificial membrane HPLC in drug research, *J Med Chem 46*, 655-665.

14. Smith, R. N., Hansch, C., and Ames, M. M. (1975) Selection of a Reference Partitioning System for Drug Design Work, *J Pharm Sci-Us 64*, 599-606.

15. Austin, R. P., Davis, A. M., and Manners, C. N. (1995) Partitioning of Ionizing Molecules between Aqueous Buffers and Phospholipid-Vesicles, *J Pharm Sci-Us 84*, 1180-1183.

16. Thurnhofer, H., Schnabel, J., Betz, M., Lipka, G., Pidgeon, C., and Hauser, H. (1991) Cholesterol-Transfer Protein Located in the Intestinal Brush-Border Membrane - Partial-Purification and Characterization, *Biochim Biophys Acta 1064*, 275-286.

17. Liu, X. L., Tanaka, H., Yamauchi, A., Testa, B., and Chuman, H. (2005) Determination of lipophilicity by reversed-phase high-performance liquid chromatography - Influence of 1-octanol in the mobile phase, *J Chromatogr A 1091*, 51-59.

18. Quinn, P. J. (1976) The Molecular Biology of Cell Membranes, Macmillan, London.

19. Hillgren, K. M., Kato, A., and Borchardt, R. T. (1995) In-Vitro Systems for Studying Intestinal Drug Absorption, *Med Res Rev 15*, 83-109.

20. Kansy, M., Senner, F., and Gubernator, K. (1998) Physicochemical high throughput screening: Parallel artificial membrane permeation assay in the description of passive absorption processes, *J Med Chem 41*, 1007-1010.

21. Walter, A., and Gutknecht, J. (1984) Monocarboxylic Acid Permeation through Lipid Bilayer-Membranes, *J Membrane Biol 77*, 255-264.

22. Balon, K., Riebesehl, B. U., and Muller, B. W. (1999) Drug liposome partitioning as a tool for the prediction of human passive intestinal absorption, *Pharm Res 16*, 882-888.

23. Kaliszan, R. (1992) Quantitative Structure-Retention Relationships, *Anal Chem 64*, A619-&.

24. Chen, B. K., and Horvath, C. (1979) Evaluation of Substituent Contributions to Chromatographic Retention - Quantitative Structure-Retention Relationships, *J Chromatogr 171*, 15-28.

25. Krikorian, S. E., Chorn, T. A., and King, J. W. (1987) Determination of Octanol Water Partition-Coefficients of Certain Organophosphorus Compounds Using High-Performance Liquid-Chromatography, *Quant Struct-Act Rel 6*, 65-69.

26. Yamagami, C., Yokota, M., and Takao, N. (1994) Hydrophobicity Parameters Determined by Reversed-Phase Liquid-Chromatography .8. Hydrogen-Bond Effects of Ester and Amide Groups in Heteroaromatic-Compounds on the Relationship between the Capacity Factor and the Octanol-Water Partition-Coefficient, *J Chromatogr A 662*, 49-60.

27. Barbato, F., Cappello, B., Miro, A., La Rotonda, M. I., and Quaglia, F. (1998) Chromatographic indexes on immobilized artificial membranes for the prediction of transdermal transport of drugs, *Farmaco 53*, 655-661.

28. Beigi, F., Gottschalk, I., Hagglund, C. L., Haneskog, L., Brekkan, E., Zhang, Y. X., Osterberg, T., and Lundahl, P. (1998) Immobilized liposome and biomembrane partitioning chromatography of drugs for prediction of drug transport, *Int J Pharmaceut 164*, 129-137.

29. Gulati, M., Grover, M., Singh, S., and Singh, M. (1998) Lipophilic drug derivatives in liposomes, *Int J Pharmaceut 165*, 129-168.

30. Banerjee, R. (2001) Liposomes: Applications in medicine, *J Biomater Appl 16*, 3-21.

31. Gregoriadis, G. (1995) Engineering liposomes for drug delivery: progress and problems, *Trends in Biotechnology 13*, 527-537.

32. Gabizon, A., Dagan, A., Goren, D., Barenholz, Y., and Fuks, Z. (1982) Liposomes as Invivo Carriers of Adriamycin - Reduced Cardiac Uptake and Preserved Anti-Tumor Activity in Mice, *Cancer Res 42*, 4734-4739.

33. Olson, F., Mayhew, E., Maslow, D., Rustum, Y., and Szoka, F. (1982) Characterization, Toxicity and Therapeutic Efficacy of Adriamycin Encapsulated in Liposomes, *Eur J Cancer Clin On 18*, 167-&.

34. Stamp, D., and Juliano, R. L. (1979) Factors Affecting the Encapsulation of Drugs within Liposomes, *Can J Physiol Pharm 57*, 535-539.

35. Fahr, A., van Hoogevest, P., May, S., Bergstrand, N., and Leigh, M. L. S. (2005) Transfer of lipophilic drugs between liposomal membranes and biological interfaces: Consequences for drug delivery, *Eur J Pharm Sci 26*, 251-265.

36. Hunt, C. A. (1982) Liposomes Disposition Invivo .5. Liposome Stability in Plasma and Implications for Drug Carrier Function, *Biochim Biophys Acta 719*, 450-463.

37. Van Etten, E. W. M., Stearne-Cullen, L. E. T., Ten Kate, M. T., and Bakker-Woudenberg, I. A. J. M. (2000) Efficacy of liposomal amphotericin B with prolonged circulation in blood in treatment of severe pulmonary aspergillosis in leukopenic rats, *Antimicrob Agents Ch 44*, 540-545.

38. Killion JJ, F. I. (1994) Systemic targeting of liposome-encapsulated immunomodulators to macrophages for treatment of cancer metastasis., *Immunomethods 4*, 273-279.

39. Sapra, P., and Allen, T. M. (2003) Ligand-targeted liposomal anticancer drugs, *Prog Lipid Res 42*, 439-462.

40. Gotfredsen, C. F., Vanberkel, T. J. C., Kruijt, J. K., and Goethals, A. (1983) Cellular-Localization of Stable Solid Liposomes in the Liver of Rats, *Biochem Pharmacol 32*, 3389-3396.

41. Giraud, F., and Claret, M. (1979) Study of Cholesterol Transfers between Erythrocytes and Lipid Vesicles - Possible Involvement of Interparticular Collisions, *Febs Lett 103*, 186-191.

42. Jonas, A., and Maine, G. T. (1979) Kinetics and Mechanism of Phosphatidylcholine and Cholesterol Exchange between Single Bilayer Vesicles and Bovine Serum High-Density Lipoprotein, *Biochemistry-Us 18*, 1722-1728.

43. Mclean, L. R., and Phillips, M. C. (1981) Mechanism of Cholesterol and Phosphatidylcholine Exchange or Transfer between Unilamellar Vesicles, *Biochemistry-Us 20*, 2893-2900.

44. Decuyper, M., and Joniau, M. (1985) Spontaneous Intervesicular Transfer of Anionic Phospholipids Differing in the Nature of Their Polar Headgroup, *Biochim Biophys Acta 814*, 374-380.

45. Patton, G. M., Robins, S. J., Fasulo, J. M., and Clark, S. B. (1985) Influence of Lecithin Acyl Chain Composition on the Kinetics of Exchange between Chylomicrons and High-Density Lipoproteins, *J Lipid Res 26*, 1285-1293.

46. Dougherty, T. J., Potter, W. R., & Bellnier, D. (1990) *Photodynamic Therapy of Neoplastic Disease*, Vol. 1 Boston.

47. Moan, J., and Berg, K. (1992) Photochemotherapy of Cancer - Experimental Research, *Photochem Photobiol 55*, 931-948.

48. van den Bergh, H. (1998) On the evolution of some endoscopic light delivery systems for photodynamic therapy, *Endoscopy 30*, 392-407.

49. Spikes, J. D., and Straight, R. C. (1990) *Photodynamic Therapy of Neoplastic Disease*, Vol. 1, CRC Press, Boston.

50. Moan, J., and Berg, K. (1991) The Photodegradation of Porphyrins in Cells Can Be Used to Estimate the Lifetime of Singlet Oxygen, *Photochem Photobiol 53*, 549-553.

51. Berg, K., Western, A., Bommer, J. C., and Moan, J. (1990) Intracellular-Localization of Sulfonated Meso-Tetraphenylporphines in a Human Carcinoma Cell-Line, *Photochem Photobiol 52*, 481-487.

52. Oenbrink, G., Jurgenlimke, P., and Gabel, D. (1988) Accumulation of Porphyrins in Cells - Influence of Hydrophobicity Aggregation and Protein-Binding, *Photochem Photobiol 48*, 451-456.

53. Salet, C., and Moreno, G. (1990) New Trends in Photobiology - Photosensitization of Mitochondria - Molecular and Cellular Aspects, *J Photoch Photobio B 5*, 133-150.

54. Derycke, A. S. L., and de Witte, P. A. M. (2004) Liposomes for photodynamic therapy, *Adv Drug Deliver Rev 56*, 17-30.

55. Kessel, D., Morgan, A., and Garbo, G. M. (1991) Sites and Efficacy of Photodamage by Tin Etiopurpurin Invitro Using Different Delivery Systems, *Photochem Photobiol 54*, 193-196.

56. Richter, A. M., Waterfield, E., Jain, A. K., Canaan, A. J., Allison, B. A., and Levy, J. G. (1993) Liposomal Delivery of a Photosensitizer, Benzoporphyrin Derivative Monoacid Ring-a (Bpd), to Tumor-Tissue in a Mouse-Tumor Model, *Photochem Photobiol 57*, 1000-1006.

57. Zhou, C., Milanesi, C., and Jori, G. (1988) An Ultrastructural Comparative-Evaluation of Tumors Photosensitized by Porphyrins Administered in Aqueous-Solution, Bound to Liposomes or to Lipoproteins, *Photochem Photobiol 48*, 487-492.

58. Cozzani, I., Jori, G., Bertoloni, G., Milanesi, C., Carlini, P., Sicuro, T., and Ruschi, A. (1985) Efficient Photosensitization of Malignant Human-Cells Invitro by Liposome-Bound Porphyrins, *Chem-Biol Interact 53*, 131-143.

59. Jori, G., Tomio, L., Reddi, E., Rossi, E., Corti, L., Zorat, P. L., and Calzavara, F. (1983) Preferential Delivery of Liposome-Incorporated Porphyrins to Neoplastic-Cells in Tumor-Bearing Rats, *Brit J Cancer 48*, 307-309.

60. Reddi, E., Zhou, C., Biolo, R., Menegaldo, E., and Jori, G. (1990) Liposome-Administered or Ldl-Administered Zn(Ii)-Phthalocyanine as a Photodynamic Agent for Tumors .1. Pharmacokinetic Properties and Phototherapeutic Efficiency, *Brit J Cancer 61*, 407-411.

61. Jori, G., Beltramini, M., Reddi, E., Salvato, B., Pagnan, A., Ziron, L., Tomio, L., and Tsanov, T. (1984) Evidence for a Major Role of Plasma-Lipoproteins as Hematoporphyrin Carriers Invivo, *Cancer Lett 24*, 291-297.

62. Reyftmann, J. P., Morliere, P, Goldstein, S., Santus, R., Dubertret, L., and Lagrange, D. . (1984) INTERACTION OF HUMAN SERUM LOW DENSITY LIPOPROTEINS WITH PORPHYRINS: A SPECTROSCOPIC AND PHOTOCHEMICAL STUDY, *Photochem Photobiol 40*, 721-730.

63. Moan, J., Smedshammer, L., and Christensen, T. (1980) Photodynamic Effects on Human-Cells Exposed to Light in the Presence of Hematoporphyrin - Ph Effects, *Cancer Lett 9*, 327-332.

64. Brault, D., Veverbizet, C., and Ledoan, T. (1986) Spectrofluorimetric Study of Porphyrin Incorporation into Membrane Models - Evidence for Ph Effects, *Biochim Biophys Acta 857*, 238-250.

65. Peng, Q., Moan, J., and Cheng, L. S. (1991) The Effect of Glucose-Administration on the Uptake of Photofrin-Ii in a Human Tumor Xenograft, *Cancer Lett 58*, 29-35.

66. Thomas, J. P., and Girotti, A. W. (1989) Glucose-Administration Augments Invivo Uptake and Phototoxicity of the Tumor-Localizing Fraction of Hematoporphyrin Derivative, *Photochem Photobiol 49*, 241-247.

67. Fugler, L., Clejan, S., and Bittman, R. (1985) Movement of Cholesterol between Vesicles Prepared with Different Phospholipids or Sizes, *J Biol Chem 260*, 4098-4102.

68. Thomas, R. M., Baici, A., Werder, M., Schulthess, G., and Hauser, H. (2002) Kinetics and mechanism of long-chain fatty acid transport into phosphatidylcholine vesicles from various donor systems, *Biochemistry-Us 41*, 1591-1601.

69. Shulok, J. R., Wade, M. H., and Lin, C. W. (1990) Subcellular-Localization of Hematoporphyrin Derivative in Bladder-Tumor Cells in Culture, *Photochem Photobiol 51*, 451-457.

70. Mojzisova, H., Bonneau, S., and Brault, D. (2007) Structural and physico-chemical determinants of the interactions of macrocyclic photosensitizers with cells, *Eur Biophys J Biophy 36*, 943-953.

71. Bonnett, R., White, R. D., Winfield, U. J., and Berenbaum, M. C. (1989) Hydroporphyrins of the Meso-Tetra(Hydroxyphenyl)Porphyrin Series as Tumor Photosensitizers, *Biochem J 261*, 277-280.

72. Biel, M. A. (2002) Photodynamic therapy in head and neck cancer, *Curr. Oncol. Rep 4*, 87-96.

73. Kubler, A. C., Haase, T., Staff, C., Kahle, B., Rheinwald, M., and Muhling, J. (1999) Photodynamic therapy of primary nonmelanomatous skin tumours of the head and neck, *Laser Surg Med 25*, 60-68.

74. Fahr, A., and Seelig, J. (2001) Liposomal formulations of cyclosporin A: A biophysical approach to pharmacokinetics and pharmacodynamics, *Crit Rev Ther Drug 18*, 141-172.

75. Meindl, W. R., Vonangerer, E., Schonenberger, H., and Ruckdeschel, G. (1984) Benzylamines - Synthesis and Evaluation of Antimycobacterial Properties, *J Med Chem 27*, 1111-1118.

76. Lombardo, F., Shalaeva, M. Y., Tupper, K. A., Gao, F., and Abraham, M. H. (2000) ElogP(oct): A tool for lipophilicity determination in drug discovery, *J Med Chem 43*, 2922-2928.

77. Liu, X. L., Tanaka, H., Yamauchi, A., Testa, B., and Chuman, H. (2004) Lipophilicity measurement by reversed-phase high-performance liquid chromatography (RP-HPLC): A comparison of two stationary phases based on retention mechanisms, *Helv Chim Acta 87*, 2866-2876.

78. Kamlet, M. J., Abboud, J. L. M., Abraham, M. H., and Taft, R. W. (1983) Linear Solvation Energy Relationships .23. A Comprehensive Collection of the Solvatochromic Parameters, Pi-Star, Alpha and Beta, and Some Methods for Simplifying the Generalized Solvatochromic Equation, *J Org Chem 48*, 2877-2887.

79. Abraham, M. H. (1993) Scales of Solute Hydrogen-Bonding - Their Construction and Application to Physicochemical and Biochemical Processes, *Chem Soc Rev 22*, 73-83.

80. Kamlet, M. J., Doherty, R. M., Abraham, M. H., Marcus, Y., and Taft, R. W. (1988) Linear Solvation Energy Relationships .46. An Improved Equation for Correlation and Prediction of Octanol Water Partition-Coefficients of Organic Nonelectrolytes (Including Strong Hydrogen-Bond Donor Solutes), *J Phys Chem-Us 92*, 5244-5255.

81. Eltayar, N., Tsai, R. S., Testa, B., Carrupt, P. A., and Leo, A. (1991) Partitioning of Solutes in Different Solvent Systems - the Contribution of Hydrogen-Bonding Capacity and Polarity, *J Pharm Sci-Us 80*, 590-598.

82. Steyaert, G., Lisa, G., Gaillard, P., Boss, G., Reymond, F., Girault, H. H., Carrupt, P. A., and Testa, B. (1997) Intermolecular forces expressed in 1,2-dichloroethane-water partition coefficients - A solvatochromic analysis, *J Chem Soc Faraday T 93*, 401-406.

83. Macdonald, R. C., Macdonald, R. I., Menco, B. P. M., Takeshita, K., Subbarao, N. K., and Hu, L. R. (1991) Small-Volume Extrusion Apparatus for Preparation of Large, Unilamellar Vesicles, *Biochim Biophys Acta 1061*, 297-303.

84. Hellings, J. A., Kamp, H. H., Wirtz, K. W. A., and Vandeene.Ll. (1974) Transfer of Phosphatidylcholine between Liposomes, *Eur J Biochem 47*, 601-605.

85. A. M. H. P. Van den Besselaar, G. M. H. J., K. W. A. Wirtz. (1975) Kinetic model of the protein-mediated phosphatidylcholine exchange between single bilayer liposomes, *Biochemistry-Us 14*, 1852-1858.

86. Bioloom version 1, B. C., Clarement, CA.

87. Taillardat-Bertschinger, A., Martinet, C. A. M., Carrupt, P. A., Reist, M., Caron, G., Fruttero, R., and Testa, B. (2002) Molecular factors influencing retention on immobilized artifical membranes (IAM) compared to partitioning in liposomes and n-octanol, *Pharm Res 19*, 729-737.

88. C. A. Marca Martinet, P. D. T., University of Lausanne, 2001.

89. Tomida, H., Yotsuyanagi, T., and Ikeda, K. (1978) Solubilization of Steroid-Hormones by Polyoxyethylene Lauryl Ether, *Chem Pharm Bull 26*, 2832-2837.

90. Barbato, F., di Martino, G., Grumetto, L., and La Rotonda, M. I. (2005) Can protonated beta-blockers interact with biomembranes stronger than neutral isolipophilic compounds? A chromatographic study on three different phospholipid stationary phases (IAM-HPLC), *Eur J Pharm Sci 25*, 379-386.

91. Avdeef, A., Box, K. J., Comer, J. E. A., Hibbert, C., and Tam, K. Y. (1998) pH-metric logP 10. Determination of liposomal membrane-water partition coefficients of ionizable drugs, *Pharm Res 15*, 209-215.

92. Barbato, F., di Martino, G., Grumetto, L., and La Rotonda, M. I. (2004) Prediction of drug-membrane interactions by IAM-HPLC: effects of different phospholipid stationary phases on the partition of bases, *Eur J Pharm Sci 22*, 261-269.

93. Barbato, F., LaRotonda, M. I., and Quaglia, F. (1997) Interactions of nonsteroidal antiinflammatory drugs with phospholipids: Comparison between octanol/buffer

partition coefficients and chromatographic indexes on immobilized artificial membranes, *J Pharm Sci-Us 86*, 225-229.

94. Florence, A. T., Attwood, D. (2006) The solubility of drugs, In *Physicochemical Principles of Pharmacy* (Florence, A. T., Attwood, A., Ed.), pp 140-176, Pharmaceutical Press, Great Britain.

95. Liu, X. L., Bouchard, G., Muller, N., Galland, A., Girault, H., Testa, B., and Carrupt, P. A. (2003) Solvatochromic analysis of partition coefficients in the o-nitrophenyl octyl ether (o-NPOE)/water system, *Helv Chim Acta 86*, 3533-3547.

96. Geinoz S. Ph.D. Thesis, U. o. L., 2002.

97. Xiangli Liu., H. T., Aiko Yamauchi., Bernard Testa., Hiroshi Chuman. (2004) Lipophilicity measurement by RP-HPLC: A comparison of two stationary phases based on retention mechanisms, *Helv. Chim. Acta 87*, 2866-2876.

98. Chen, J. Y., Mak, N. K., Yow, C. M. N., Fung, M. C., Chiu, L. C., Leung, W. N., and Cheung, N. H. (2000) The binding characteristics and intracellular localization of temoporfin (mTHPC) in myeloid leukemia cells: Phototoxicity and mitochondrial damage, *Photochem Photobiol 72*, 541-547.

99. Ricchelli, F., Jori, G., Gobbo, S., and Tronchin, M. (1991) Liposomes as Models to Study the Distribution of Porphyrins in Cell-Membranes, *Biochim Biophys Acta 1065*, 42-48.

100. Jones, J. D., and Thompson, T. E. (1989) Spontaneous Phosphatidylcholine Transfer by Collision between Vesicles at High Lipid-Concentration, *Biochemistry-Us 28*, 129-134.

101. Steck, T. L., Kezdy, F. J., and Lange, Y. (1988) An Activation-Collision Mechanism for Cholesterol Transfer between Membranes, *J Biol Chem 263*, 13023-13031.

102. Lange, Y., Molinaro, A. L., Chauncey, T. R., and Steck, T. L. (1983) On the Mechanism of Transfer of Cholesterol between Human-Erythrocytes and Plasma, *J Biol Chem 258*, 6920-6926.

103. Schulthess, G., Lipka, G., Compassi, S., Boffelli, D., Weber, F. E., Paltauf, F., and Hauser, H. (1994) Absorption of Monoacylglycerols by Small-Intestinal Brush-Border Membrane, *Biochemistry-Us 33*, 4500-4508.

104. Kuntsche, J., Freisleben, I., Steiniger, F., and Fahr, A. (2010) Temoporfin-loaded liposomes: Physicochemical characterization, *Eur J Pharm Sci 40*, 305-315.

105. Wenk, M. R., Fahr, A., Reszka, R., and Seelig, J. (1996) Paclitaxel partitioning into lipid bilayers, *J Pharm Sci-Us 85*, 228-231.

106. Dill, K. A., and Stigter, D. (1988) Lateral Interactions among Phosphatidylcholine and Phosphatidylethanolamine Head Groups in Phospholipid Monolayers and Bilayers, *Biochemistry-Us 27*, 3446-3453.

107. Jain, M. K., and Zakim, D. (1987) The Spontaneous Incorporation of Proteins into Preformed Bilayers, *Biochim Biophys Acta 906*, 33-68.

108. Wright, S. E., White, J. C., and Huang, L. (1990) Partitioning of Teniposide into Membranes and the Role of Lipid-Composition, *Biochim Biophys Acta 1021*, 105-113.

109. Scherer, P. G., and Seelig, J. (1989) Electric Charge Effects on Phospholipid Headgroups - Phosphatidylcholine in Mixtures with Cationic and Anionic Amphiphiles, *Biochemistry-Us 28*, 7720-7728.

110. Zantl, R., Baicu, L., Artzner, F., Sprenger, I., Rapp, G., and Radler, J. O. (1999) Thermotropic phase behavior of cationic lipid-DNA complexes compared to binary lipid mixtures, *J Phys Chem B 103*, 10300-10310.

111. Jurkiewicz, P., Olzynska, A., Langner, M., and Hof, M. (2006) Headgroup hydration and mobility of DOTAP/DOPC bilayers: A fluorescence solvent relaxation study, *Langmuir 22*, 8741-8749.

112. Gurtovenko, A. A., Patra, M., Karttunen, M., and Vattulainen, I. (2004) Cationic DMPC/DMTAP lipid bilayers: Molecular dynamics study, *Biophys J 86*, 3461-3472.

113. Mbamala, E. C., Fahr, A., and May, S. (2006) Electrostatic model for mixed cationic-zwitterionic lipid bilayers, *Langmuir 22*, 5129-5136.

114. Mengistu, D. H., and May, S. (2008) Nonlinear Poisson-Boltzmann model of charged lipid membranes: Accounting for the presence of zwitterionic lipids, *J Chem Phys 129*, 121105.

115. Jenning, V., Schafer-Korting, M., and Gohla, S. (2000) Vitamin A-loaded solid lipid nanoparticles for topical use drug release properties, *J Control Release 66*, 115-126.

116. Jores, K., Mehnert, W., and Mader, K. (2003) Physicochemical investigations on solid lipid nanoparticles and on oil-loaded solid lipid nanoparticles: A nuclear magnetic resonance and electron spin resonance study, *Pharm Res 20*, 1274-1283.

117. Fahr, A., and Liu, X. (2007) Drug delivery strategies for poorly water-soluble drugs, *Expert Opin Drug Del 4*, 403-416.

118. Maman, N., and Brault, D. (1998) Kinetics of the interactions of a dicarboxylic porphyrin with unilamellar lipidic vesicles: interplay between bilayer thickness and pH in rate control, *Bba-Biomembranes 1414*, 31-42.

Selbstständigkeitserklärung:

Hiermit erkläre ich Hossam Hefesha, dass ich die vorliegende Arbeit selbstständig und nur unter Verwendung der angegebenen Hilfsmittel und Literatur angefertigt habe. Das mathematische Modell in der Anlage wurde von Prof. Dr.Sylvio May geschaffen.

Hossam Hefesha

Jena, den 23.11.2010

Supervision of undergraduate students in practical course, 3rd semester, in pharmaceutical technology department, Friedrich Schiller University, Jena, Germany (2007-2009).

Lab experiences:

Preparation of different pharmaceutical formulations like liposomes, emulsions, suspensions, tablets and suppositories.

Researches in pharmacokinetics and biopharmaceutics of different Formulations.

Drug release kinetics from liposomal preparations by different techniques.

HPLC managing.

Courses:

Preparatory courses:

In Organic Chemistry, Mathematics, Statistics, computer science, English, Physical Chemistry and Instrumental Analysis.

Special courses:

In: Physical Pharmacy, Industrial Pharmacy, Preformulation studies, Bioavailability.

Language skills:

Arabic: Native

English: Very good

German: Good

Publications:

1- Hossam Hefesha, Stephan Loew, Xiangli Liu, Sylvio May and Alfred Fahr: Transfer Mechanism of Temoporfin between Liposomal Membranes (Journal of Controlled Release, in press).

2- Liu, X., Fan, P., Chen, M., Hefesha, H., Scriba, G.K.E., Gabel, D. & Fahr, A.: Drug-membrane interaction on immobilized liposome chromatography compared to immobilized artificial membrane (IAM), liposome/water and n-octanol/water systems, Helvetica Chimica Acta – Vol. 93 (2010).

3- Liu, X., Hefesha, H., Tanaka, H., Scriba, G. & Fahr, A.: Lipophilicity Measurement of Drugs by Reversed Phase HPLC over Wide pH Range Using an Alkaline-Resistant Silica-Based Stationary Phase, XBridgeTM Shield RP18, Chem. Pharm. Bull., 56, 1417-1422, 2008 ***(Equal contribution as first author)*.**

4- Liu, X., Hefesha, H., Scriba, G. & Fahr, A. Retention behavior of neutral, positively and negatively charged solutes on immobilized artificial membrane (IAM) stationary phase, Helv. Chim. Acta, 91, 1505-1512, 2008 ***(Equal contribution as first author)***.

Conferences Contributions:

1- Al-Azhar 4th-International Conference for Pharmaceutical & Biological Science, February, 13-15, 2006.

A- Preliminary investigation and in-vitro release of diclofenac sodium microspheres (Poster1).
B- Statistical correlation and factorial characterization of diclofenac sodium microspheres (Poster2).

2- Controlled Release Society (CRS) German Chapter annual Meeting, Halle (Saale), March 19th-20th, 2009. Cholesterol transfer (exchange) between liposomal membranes. (Poster)

3- Deutschen Pharmazeutischen Gesellschaft, Jena, September 28th-1st October, 2009. Kinetics of a hydrophobic drug (temoporfin; mTHPC) transfer between liposomal membranes. (Poster)

Interest:

Reading, soccer games, swimming, and table tennis.

Present Address:

August Bebel Straße 27A, 07743-Jena, Germany.